a result of inefficient transduction of the hematopoietic stem cells by the retroviral vectors.

Lentiviral vectors have been developed to overcome this inefficiency [7], with resultant transduction and integration of therapeutic genes into the target genome [4–6]. The commonly used lentiviral vectors are derived from HIV-1 or HIV-2 and endeavors have been made to make lentiviral vectors much safer [27]. However, the pathogenicity of HIV-based lentiviral vectors to humans is not clear especially in HIV carriers. Therefore, use of these vectors raises safety issues. The safety of HIV-derived vectors ultimately must be proven, but remains difficult because of the limited availability of animal models of HIV-induced diseases. The SIV lentiviral vectors used in this study were derived from SIVagmTYO1, non-pathogenic to its natural hosts or to experimentally infected Asian macaques [8], and no replication-competent virus particles were detected in vector-infected cells *in vitro*. Furthermore, the risk of development of replication-competent lentivirus particles in HIV carrier patients may be significantly lower than that for the HIV-1-based vectors because of the low sequence homology between HIV-1 and SIVagmTYO1. In this regard, SIVagmTYO1-based vectors have an advantage regarding safety issues and clinical application of gene therapy. To our knowledge, this is the first report of stable production of human FVIII in mice by hematopoietic cells reconstituted from CB-CD34$^+$ cells transduced with SIV vectors.

In the current study, the transduction efficiency of the CB-CD34$^+$ cells with the SIV vectors (Figure 1) was comparable to HIV-based lentiviral vectors [4]. Production of hFVIII (274.3 ± 20.1 ng/10^6 cells/24 h) by transduced CB-CD34$^+$ cells *in vitro* was considerable, raising the possibility of achieving therapeutic levels of plasma FVIII in the mice. After engraftment of transduced cells in NOD/SCID mice, plasma FVIII levels were maximal at 3.6 ± 0.8 ng/mL on day 6 after transplantation, declining gradually to a sustained level of 1.2 ng/mL for at least 60 days. The hFVIII production was observed in plasma and at the gene level in bone marrow cells. The hFVIII levels in plasma were lower than expected based on the *in vitro* production rate. One contributing factor may be the shorter half-life of hFVIII in mice compared with humans. The half-life of injected hFVIII in mice is approximately 1 h, whereas the half-life in hemophilia patients is closer to 8–12 h [25]. Chao *et al.* showed low-level production of hFVIII in immunocompetent C57BL/6 mice expressing a hFVIII inhibitor or in NOD/SCID mice without a detectable inhibitor. In these studies, FVIII levels increased after 10 months in both mice populations at the disappearance time of the inhibitor in the C57BL/6 mice [28]. Thus, secreted hFVIII was likely degraded in the NOD/SCID mice, analogous to that observed in the immunocompetent mice, resulting in low circulating levels of FVIII. It is also possible that the number of FVIII-producing cells decreased gradually after transplantation. We incubated CB-CD34$^+$ cells with SIVhFVIII at MOI of 50 vg/cell and approximately 50% of the CB-CD34$^+$ cells were transduced. These cells consist of hematopoietic stem cells and hematopoietic progenitor cells. During the early period after transplantation, the transduced cells produced hFVIII, as reflected by the relatively high level of plasma hFVIII in mice on days 1 and 6 after transplantation. After day 6, transduced human hematopoietic progenitor cells may have differentiated to progeny cells, which would be liberated from the bone marrow and cleared. Thus, the number of hFVIII-producing cells might be decreased after day 6 as they are derived solely from transduced human hematopoietic stem cells, their progeny and differentiated cells. The expected result would be declining plasma FVIII levels in the later periods of post-transplantation. It is also possible that silencing of the CMV promoter *in vivo* could have occurred, that in turn reduced FVIII production. The FVIII levels achieved in mice in this study were relatively low but such an increase of the FVIII level would develop clinical effects in hemophilias such as decrease of bleeding episodes and of use of FVIII concentrates. Data on clinical trials of hemophilia A gene therapy support this notion [29,30]. Therefore, we think that the FVIII levels achieved in this study were relatively low but an increase of FVIII to these levels would develop clinical improvement in severe hemophilia patients.

The replication mechanism of HIV-1 has been extensively studied in host cells. HIV-1 has the unique property among retroviruses to replicate in non-dividing cells. This property enables HIV-1 and other lentiviral-based vectors to transduce non-dividing hematopoietic stem cells. The central DNA flap of HIV-1 is thought to function as a cis-determinant of HIV-1 DNA nuclear import and to play a crucial role for lentiviral vector nuclear import and gene transduction of hematopoietic stem cells [31,32]. The SIVagm vectors used in this study were developed essentially according to the HIV-1-based vectors. Although SIVagm vectors are self-inactivating type vectors, the central DNA flap has not been included in the vectors as yet. We were able to transduce CD34$^+$ cells using SIVagm vectors efficiently *in vitro*, as shown in Figure 1, but FVIII production was decreased after transplantation. Thus, transgene integration into the CD34$^+$ cell genome by the SIVagmTYO1 vector might not occur efficiently. Currently, we are redesigning the SIVagmTYO1 vector to include the DNA flap. Use of such third-generation SIVagmTYO1 vectors will be of interest in future studies.

Analyses of lineage marker expression on the hematopoietic cells from the bone marrow and spleen of NOD/SCID mice confirmed engraftment and hematopoiesis of the transduced cells in the mice. Furthermore, we demonstrated CD41$^+$ platelets in the peripheral blood and the bone marrow, indicating that the human megakaryocytic progenitors could differentiate and mature to produce platelets in the mice. In fact, 2 ng of human FVIII were detected by ELISA in the platelet extracts derived from 1 mL of recipient mouse peripheral blood. These data also suggest that this is another advantage of transplantation of FVIII-producing hematopoietic stem cells, since the FVIII can be stored in platelets. These

platelets circulate in blood and secrete FVIII upon platelet activation in the vicinity of bleeding, so that local FVIII concentrations may be higher than that in the circulation.

We demonstrated efficient transduction of CB-CD34$^+$ cells by a SIV vector carrying the human FVIII gene. Taking advantage of their self-renewal and multi-lineage differentiation capabilities, transplantation of *ex vivo* engineered CB-CD34$^+$ cells enabled their engraftment in NOD/SCID mice, transgene expression, and human FVIII production. Because of xenograft transplantation, we transplanted human CD34$^+$ cells to NOD/SCID mice with myeloablation by irradiation. However, this gene therapy strategy can be potentially applicable to clinical studies because autologous transplantation of genetically transduced hematopoietic stem cells can be achieved with non-myeloablative conditioning [33]. Transplantation of *ex vivo* SIV vector-transduced CD34$^+$ cells without exposure of subjects to viral vectors is a useful approach with potential clinical application for gene therapy of hemophilia patients.

Gene therapy of human ADA-SCID and X-SCID by autologous transplantation of genetically modified hematopoietic stem cells has been shown to be very effective [33,34]. However, a leukemia-like disorder emerged in two X-SCID patients who received retrovirally mediated common $\gamma(\gamma c)$ gene transfer to hematopoietic stem cells [35]. This disorder appeared to be caused by insertion of the vector-derived γc gene in the LMO2 gene [35]. Similar to retrovirus vector-mediated gene transfer, random integration of the transgene to hematopoietic stem cell genomes takes place upon transduction by lentiviral vectors. Thus, vector-derived DNA insertion to such a leukemia-linked gene LMO2 can also happen in SIV vector-mediated FVIII gene transfer to hematopoietic stem cells. The SIV vector used in this study is designed to be a self-inactivating type vector to minimize activation of genes in the vicinity of the integration site. Thus FVIII gene transfer to hematopoietic stem cells by SIVhFVIII may be much safer than retrovirally mediated γc gene transfer to hematopoietic stem cells for X-SCID gene therapy. However, the risk of the inactivation of tumor suppressor genes still remains. Therefore, attempts such as the use of a regulated and cell-specific promoter, reduction of multiple insertion of the transgene into a single cell, and incorporation of a suicide gene into the vector should be studied to reduce the risk of development of an unpredictable disorder in the future.

Acknowledgements

We thank Dr. J. A. van Mourik for the full-length FVIII cDNA, Dr. Koichiro Tsuji, the Institute of Medical Science, the University of Tokyo, and Dr. Mika Wada, the Department of Pediatrics, Nihon University of Medicine, for advice on transplantation of human CB-CD34$^+$ cells into NOD/SCID mice. We also thank Ms. Fumino Muroi and Ms. Kou Kosaka for technical assistance with the human FVIII ELISA assay and purification of CB-CD34$^+$ cells. This work is supported in part by Health and Labour Sciences Research Grants from the Ministry of Health, Labour and Welfare and Grants-in-aid for Scientific Research from the Ministry of Education and Science. This manuscript was edited by IdEst, Inc.

References

1. Hoyer LW. Hemophilia A. *N Engl J Med* 1994; **330**: 38–47.
2. Kay MA, High K. Gene therapy for the hemophilias. *Proc Natl Acad Sci U S A* 1999; **96**: 9973–9975.
3. Kume A, Hanazono Y, Mizukami H, Urabe M, Ozawa K. Hematopoietic stem cell gene therapy: a current overview. *Int J Hematol* 1999; **68**: 227–233.
4. Miyoshi H, Smith KA, Mosier DE, Verma IM, Torbett BE. Transduction of human CD34+ cells that mediate long-term engraftment of NOD/SCID mice by HIV vector. *Science* 1999; **283**: 682–686.
5. Woods NB, Fahlman C, Mikkola H, *et al.* Lentiviral gene transfer into primary and secondary NOD/SCID repopulating cells. *Blood* 2000; **96**: 3725–3733.
6. Scherr M, Battmer K, Blomer U, *et al.* Lentiviral gene transfer into peripheral blood-derived CD34$^+$ NOD/SCID-repopulating cells. *Blood* 2002; **99**: 709–712.
7. Naldini L, Blomer U, Gallay P, *et al.* In vivo gene delivery and stable transduction of nondividing cells by a lentiviral vector. *Science* 1996; **272**: 263–267.
8. Honjo S, Narita T, Kobayashi R, *et al.* Experimental infection of African green monkeys and cynomolgus monkeys with a SIVAGM strain isolated from a healthy African green monkey. *J Med Primatol* 1990; **19**: 9–20.
9. Nakajima T, Nakamaru K, Ido E, Terao K, Hayami M, Hasegawa M. Development of novel simian immunodeficiency virus vectors carrying a dual gene expression system. *Hum Gene Ther* 2000; **11**: 1863–1874.
10. Hoeben RC, Einerhand MP, Briet E, van Ormondt H, Valerio D, van der Eb AJ. Toward gene therapy in haemophilia A: retrovirus-mediated transfer of a factor VIII gene into murine haematopoietic progenitor cells. *Thromb Haemost* 1992; **67**: 341–345.
11. Tonn T, Herder C, Becker S, Seifried E, Grez M. Generation and characterization of human hematopoietic cell lines expressing factor VIII. *J Hematother Stem Cell Res* 2002; **11**: 695–704.
12. Kootstra NA, Matsumura R, Verma IM. Efficient production of human FVIII in hemophilic mice using lentiviral vectors. *Mol Ther* 2003; **7**: 623–631.
13. Tiede A, Eder M, von Depka M, *et al.* Recombinant factor VIII expression in hematopoietic cells following lentiviral transduction. *Gene Ther* 2003; **10**: 1917–1925.
14. Ogata K, Mimuro J, Kikuchi J, *et al.* Expression of human coagulation factor VIII in adipocytes transduced with the simian immunodeficiency virus agmTYO1-based vector for haemophilia A gene therapy. *Gene Ther* 2004; **11**: 253–259.
15. Furukawa Y, Kikuchi J, Nakamura M, Iwase S, Yamada H, Matsuda M. Lineage-specific regulation of cell cycle control gene expression during haematopoietic cell differentiation. *Br J Haematol* 2000; **110**: 663–673.
16. Ueda T, Tsuji K, Yoshino H, *et al.* Expansion of human NOD/SCID-repopulating cells by stem cell factor, Flk2/Flt3 ligand, thrombopoietin, IL-6, and soluble IL-6 receptor. *J Clin Invest* 2000; **105**: 1013–1021.
17. Yoshino H, Ueda T, Kawahata M, *et al.* Natural killer cell depletion by anti-asialo GM1 antiserum treatment enhances human hematopoietic stem cell engraftment in NOD/Shi-scid mice. *Bone Marrow Transplant* 2000; **26**: 1211–1216.
18. Ma F, Wada M, Yoshino H, *et al.* Development of human lymphohematopoietic stem and progenitor cells defined by expression of CD34 and CD81. *Blood* 2001; **97**: 3755–3762.
19. Yonemura H, Sugawara K, Nakashima K, Nakahara Y, Hamamoto T, Mimaki I. Production of recombinant human factor VIII by co-expression of the heavy and light chains. *Protein Eng* 1993; **6**: 669–674.
20. Chomczynski P, Sacchi N. Single-step method of RNA isolation by acid guanidinium thiocyanate-phenol-chloroform extraction. *Anal Biochem* 1987; **162**: 156–159.
21. Sutton RE, Reitsma MJ, Uchida N, Brown PO. Transduction of human progenitor hematopoietic stem cells by human immunodeficiency virus type 1-based vectors is cell cycle dependent. *J Virol* 1999; **73**: 3649–3660.

22. Xu R, Reems JA. Umbilical cord blood progeny cells that retain a CD34+ phenotype after ex vivo expansion have less engraftment potential than unexpanded CD34+ cells. *Transfusion* 2001; **41**: 213–218.
23. VandenDriessche T, Vanslembrouck V, Goovaerts I, *et al.* Long-term expression of human coagulation factor VIII and correction of hemophilia A after in vivo retroviral gene transfer in factor VIII-deficient mice. *Proc Natl Acad Sci U S A* 1999; **96**: 10379–10384.
24. Hoeben RC, Fallaux FJ, Van Tilburg NH, *et al.* Toward gene therapy for hemophilia A: long-term persistence of factor VIII-secreting fibroblasts after transplantation into immunodeficient mice. *Hum Gene Ther* 1993; **4**: 179–186.
25. Dwarki VJ, Belloni P, Nijjar T, *et al.* Gene therapy for hemophilia A: production of therapeutic levels of human factor VIII in vivo in mice. *Proc Natl Acad Sci U S A* 1995; **92**: 1023–1027.
26. Chuah MK, Van Damme A, Zwinnen H, *et al.* Long-term persistence of human bone marrow stromal cells transduced with factor VIII-retroviral vectors and transient production of therapeutic levels of human factor VIII in nonmyeloablated immunodeficient mice. *Hum Gene Ther* 2000; **11**: 729–738.
27. Naldini L, Verma IM. Lentiviral vectors. *Adv Virus Res* 2000; **55**: 599–609.
28. Chao H, Walsh CE. Induction of tolerance to human factor VIII in mice. *Blood* 2001; **97**: 3311–3312.
29. Roth DA, Tawa NE Jr, Proper JA, *et al.* The factor VIII transkaryotic therapy study group. Nonviral transfer of the gene encoding coagulation factor VIII in patients with severe hemophilia A. *N Engl J Med* 2001; **344**: 1782–1784.
30. Powell J, Ragni MV, White GC, *et al.* Phase 1 trial of FVIII gene transfer for severe hemophilia A using a retroviral construct administered by peripheral intravenous infusion. *Blood* 2003; **102**: 2038–2045.
31. Zennou V, Petit C, Guetard D, Nerhbass U, Montagnier L, Charneau P. HIV-1 genome nuclear import is mediated by a central DNA flap. *Cell* 2000; **101**: 173–185.
32. Sirven A, Pflumio F, Zennou V, *et al.* The human immunodeficiency virus type-1 central DNA flap is a crucial determinant for lentiviral vector nuclear import and gene transduction of human hematopoietic stem cells. *Blood* 2000; **96**: 4103–4110.
33. Aiuti A, Slavin S, Aker M, *et al.* Correction of ADA-SCID by stem cell gene therapy combined with nonmyeloablative conditioning. *Science* 2002; **28**: 2410–2413.
34. Hacein-Bey-Abina S, Le Deist F, Carlier F, *et al.* Sustained correction of X-linked severe combined immunodeficiency by *ex vivo* gene therapy. *N Engl J Med* 2002; **346**: 1185–1193.
35. Hacein-Bey-Abina S, von Kalle C, Schmidt M, *et al.* A serious adverse event after successful gene therapy for X-linked severe combined immunodeficiency. *N Engl J Med* 2003; **348**: 255–256.

Thrombophilic dysfibrinogen Tokyo V with the amino acid substitution of γ Ala327Thr: formation of fragile but fibrinolysis-resistant fibrin clots and its relevance to arterial thromboembolism

Akiei Hamano, Jun Mimuro, Motonori Aoshima, Takeyoshi Itoh, Noboru Kitamura, Susumu Nishinarita, Katsuhiro Takano, Akira Ishiwata, Yuji Kashiwakura, Kazuki Niwa, Tomoko Ono, Seiji Madoiwa, Teruko Sugo, Michio Matsuda, and Yoichi Sakata

Thrombophilic dysfibrinogen Tokyo V was identified in a 43-year-old man with recurrent thromboembolism. Based on analyses of the patient fibrinogen genes, the amino acid sequence of the aberrant fibrinogen peptide, and deglycosylation experiments, fibrinogen Tokyo V was shown to have an amino acid substitution of γ Ala327Thr and possibly extra glycosylation at γ Asn325 because the mutation confers the N-linked glycosylation consensus sequence Asn-X-Thr. The mutation resulted in impaired function and hypofibrinogenemia (hypodysfibrinogen). Polymerization of fibrin monomers derived from patient fibrinogen was severely impaired with a partial correction in the presence of calcium, resulting in very low clottability. Additionally, a large amount of soluble cross-linked fibrin was formed upon thrombin treatment in the presence of factor XIII and calcium. However, Tokyo V–derived fibrin was resistant to degradation by tissue plasminogen activator (tPA)–catalyzed plasmin digestion. The structure of Tokyo V fibrin appeared severely perturbed, since there are large pores inside the tangled fibrin networks and fiber ends at the boundaries. Taken together, these data suggest that Tokyo V fibrin clots are fragile, so that fibrinolysis-resistant insoluble fibrin and soluble fibrin polymers may be released to the circulation, partly accounting for the recurrent embolic episodes in the patient. (Blood. 2004;103:3045-3050)

Introduction

Fibrinogen is a 340-kDa plasma protein that participates in the final step of blood coagulation and also plays an important role in platelet aggregation.[1,2] Fibrinogen is composed of 2 identical molecular halves, each being composed of an Aα, a Bβ, and a γ chain. These polypeptides are encoded by 3 independent genes, clustered on chromosome 4. During synthesis in the liver, these chains are translated, processed, and assembled to the mature molecules.[3] Many reports have shown that a variety of genetic mutations result in molecular defects in fibrinogen molecules (dysfibrinogen)[4,5] or decreased levels of fibrinogen in blood (afibrinogenemia and hypofibrinogenemia).[6]

Analyses of molecular and functional abnormalities of dysfibrinogens participate in elucidation of structure-function relationships and fibrin polymerization mechanisms. Patients with dysfibrinogen show bleeding tendencies, thromboembolisms, or no apparent symptoms, depending on the molecular abnormality. Thrombophilic dysfibrinogen is a rare molecular abnormality.[5] Here we report a new thrombophilic dysfibrinogen with an amino acid substitution of γ Ala327Thr, inserting a possible extra N-glycosylation site at γ Asn325. The defective fibrinogen results in formation of fragile but fibrinolysis-resistant clots caused by conformation defects in the vicinity of the "a" polymerization pocket, the high-affinity calcium ion binding site, and the tissue plasminogen activator (tPA) binding site of the γ chain.

Patients, materials, and methods

Description of the patient

A 43-year-old man, who suffered from recurrent thromboembolic episodes such as cerebral infarction at the age of 36 years and pulmonary embolism at the age of 42 years, was admitted to a hospital because of severe abdominal pain. Echography and computed tomographic (CT) scan analyses showed that thrombi were present in the thoracic and abdominal aorta and the superior mesenteric artery of the patient. The patient was suspected to have dysfibrinogen based upon coagulation studies conducted on admission. There was a marked discrepancy between fibrinogen levels in plasma determined by the thrombin time method (< 1.47 μM) and the turbidimetric method (4.00 μM) on admission. This was reproduced in another plasma sample in which there also was a discrepancy between fibrinogen levels determined by the thrombin time method (0.61 μM) and the immunologic method (2.16 μM). Thus, the patient fibrinogen was designated as fibrinogen Tokyo V. These data also suggested that the patient had not only dysfibrinogenemia, but also hypofibrinogenemia. Other coagulation studies including plasma levels of protein C, antithrombin III, plasminogen, and protein S were within normal ranges.

Analysis of purified fibrinogen

Fibrinogen was purified from plasma of healthy subjects or patient plasma as described previously.[7-10] All samples were obtained with informed consent provided by the patient according to the Declaration of Helsinki, and the study

From the Division of Cell and Molecular Medicine, Center for Molecular Medicine, Jichi Medical School, Tochigi-ken, Japan; the Department of Internal Medicine, Nihon University School of Medicine, Tokyo, Japan; and the Department of Internal Medicine, Akiru General Municipal Hospital, Tokyo, Japan.

Submitted July 30, 2003; accepted December 24, 2003. Prepublished online as *Blood* First Edition Paper, January 8, 2004; DOI 10.1182/blood-2003-07-2569.

Supported by Grants-in-Aid for Scientific Research no. 12670687 to J.M. from the Ministry of Education and Science.

An Inside *Blood* analysis of this article appears in the front of this issue.

Reprints: Jun Mimuro, Cell and Molecular Medicine, Jichi Medical School, Tochigi-ken 329-0498, Japan; e-mail: mimuro-j@jichi.ac.jp.

The publication costs of this article were defrayed in part by page charge payment. Therefore, and solely to indicate this fact, this article is hereby marked "advertisement" in accordance with 18 U.S.C. section 1734.

Table 1. Clotting times of purified fibrinogen with thrombin

	Fibrinogen Tokyo V	Normal fibrinogen
Without Ca^{2+}, s	> 300.0	11.3
With 2 mM Ca^{2+}, s	42.0	8.7

was approved by the Bioethics Committee for Gene Analysis at Jichi Medical School. Clotting of patient-derived fibrinogen was compared with normal fibrinogen by the thrombin time method in the absence or presence of calcium. The aggregation profiles of healthy subject– and patient-derived fibrin monomers were monitored at 350 nm according to the method of Gralnick as described previously.[7-10] To study effect of Tokyo V fibrin on normal fibrin polymerization, normal fibrin monomers and Tokyo V fibrin monomers at the same concentration were mixed at ratios of 9:1, 3:1, and 1:1, then processed for measuring fibrin monomer aggregation profiles as described earlier in this paragraph. For the control, normal fibrin monomers were mixed with buffer at ratios of 9:1, 3:1, and 1:1, then processed for measuring aggregation profiles of fibrin monomers. Apparent molecular mass of patient fibrinogen was analyzed by sodium dodecyl sulfate–polyacrylamide gel electrophoresis (SDS-PAGE) under reducing conditions and was compared with normal fibrinogen. Identification of the γ chain was carried out by Western blotting using γ chain–specific monoclonal antibody JIF 25 as described.[8] Purified fibrinogen (1 mg/mL) was incubated with thrombin (1 U/mL) in the absence or presence of 2 mM calcium to investigate release of fibrinopeptides A and B and the cross-linking profiles of γ chains (γ-dimer formation) and α chains (α-polymer formation) as described previously.[7-10] To assess clottability of fibrinogen, purified fibrinogen (1 mg/mL) was incubated in Tris-buffered saline containing 1 U/mL thrombin in the presence of 1 U/mL factor XIII (FXIII) and 2 mM calcium. After incubation at 37 °C for 60 minutes, fibrin clots were squeezed with bamboo sticks and the residual protein amount in supernatants was quantified by measuring absorbance at 280 nm. Relative amounts of β chain of insoluble fibrin clots and of soluble fibrin in the supernatant were quantified using a densitometer to assess the clottability of Tokyo V fibrinogen. Supernatants were analyzed by SDS-PAGE under reducing and nonreducing conditions for semiquantitation of unclotted fibrin and for analysis of soluble fibrin species.

Determination of the nucleotide sequences of fibrinogen genes

Patient genomic DNA was isolated from peripheral leukocytes by standard procedure as described previously.[7,9,10] All exons and exon-intron boundaries of fibrinogen genes were amplified by polymerase chain reaction (PCR) using Bucabest DNA polymerase (Takara, Kyoto, Japan) and appropriate primers (Invitrogen Japan, Tokyo, Japan).[10] PCR-amplified DNA fragments were isolated after agarose gel electrophoresis using a rapid gel extraction kit (Invitrogen Japan), and their nucleotide sequences were determined directly by the dideoxynucleotide termination reaction method using BigDye cycle sequencing kit and a DNA sequencer model ABI 310 (Applied Biosystems Japan, Tokyo, Japan)[10,11] or using Sequenase (US Biochemical, Cleveland, OH) and ^{35}S-dATP (Amersham Biosciences K. K., Tokyo, Japan).[7,9]

Fibrin degradation by tPA-catalyzed plasmin digestion and tPA-mediated plasmin generation

Purified fibrinogen (1 mg/mL) was incubated with tPA (1.25 U/mL), plasminogen (20 μg/mL), FXIII (1 U/mL), and thrombin (1 U/mL) in the presence of 2 mM calcium. After incubation at 37°C, the reaction was terminated by incubating samples in buffer containing 2% SDS and 10 mM dithiothreitol (DTT) at 98°C for 2 minutes and samples were analyzed by SDS-PAGE under reducing conditions. Fibrinogen (1 mg/mL), increasing concentrations of plasmin (0.3-2.4 casein U/mL), FXIII (1 U/mL), and thrombin (1 U/mL) were incubated at 37°C for 30 minutes in the presence of calcium, and fibrin degradation profiles were analyzed by SDS-PAGE as described in "Analysis of purified fibrinogen" to study Tokyo V fibrin degradation by plasmin without the plasminogen activation process by tPA. tPA-mediated plasmin generation in the presence of fibrin was studied using the synthetic plasmin substrate S-2251 as described.[8] Healthy subject or patient fibrinogen was incubated with plasminogen (20 μg/mL), tPA (4 U/mL), FXIII (1 U/mL), thrombin (1 U/mL), and S-2251 (1 mM) in the presence of 2 mM calcium in microtiter plates. Hydrolysis of S-2251 was monitored by measuring absorbance at 405 nm.

Enzymatic removal of N-linked oligosaccharides in fibrinogen

Purified fibrinogen was incubated with N-glycopeptidase F (Roche Diagnostics, Mannheim, Germany) to remove N-linked oligosaccharides in fibrinogen molecules as described previously.[9] Removal of oligosaccharides from fibrinogen molecules was confirmed by SDS-PAGE analysis. Identification of the γ chain was conducted by the Western blot analysis as described in "Analysis of purified fibrinogen."

Scanning electron microscopy of fibrin clots

To investigate the structure of Tokyo V fibrin, clots were formed on carbon-formvar–coated gold grids and processed for scanning electron microscopy using JEOL JSM6300F Field Emission Scanning Electron Microscope (Japan Electron Optics Laboratory, Tokyo, Japan) as described previously.[9]

Results

Abnormalities of purified fibrinogen Tokyo V

The clotting time of patient-derived fibrinogen (Tokyo V fibrinogen) with thrombin was remarkably prolonged to 42.0 seconds with calcium, and was not measurable in the absence of calcium (Table 1). These data confirmed that fibrinogen Tokyo V was a dysfibrinogen. Apparent mobility of purified fibrinogen Tokyo V subunit polypeptides on SDS-PAGE was indistinguishable from normal fibrinogen polypeptides (Figure 1A). There was a faint polypeptide band that migrated between the γ chain and the Bβ chain on SDS-PAGE in both the healthy subject–derived fibrinogen preparation and the patient-derived fibrinogen preparation. Western blotting analyses of purified fibrinogen preparations showed that the faint polypeptide band migrating between the γ chain and the Bβ chain in the Tokyo V fibrinogen preparation was recognized by γ chain–specific monoclonal antibody JIF25 but the band in the normal fibrinogen preparation was not, indicating the presence of a small amount of aberrant γ chain with slower mobility on SDS-PAGE in Tokyo V fibrinogen (Figure 1A). The amount of the aberrant γ chain

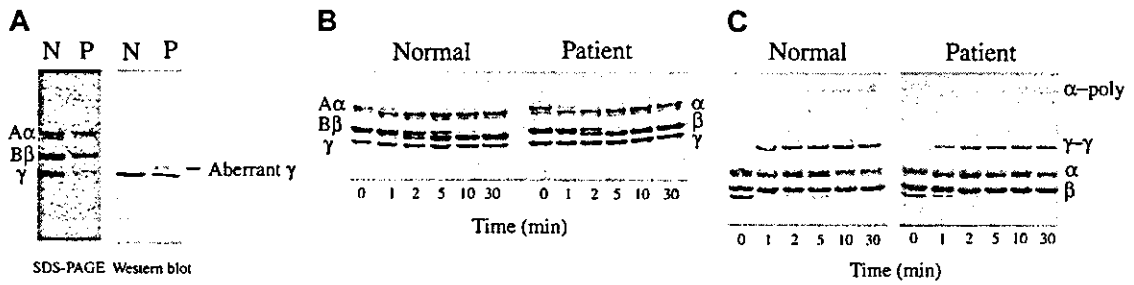

Figure 1. SDS-PAGE analysis of purified fibrinogen. Fibrinogen was purified from citrated plasma obtained from the patient (P) and healthy subjects (N) and was studied for the apparent molecular mass, the release of fibrinopeptides A and B by thrombin, and cross-linking of γ and α chains. (A) SDS-PAGE analyses (SDS-PAGE) of purified fibrinogen and identification of the γ chain by Western blotting using the γ chain–specific monoclonal antibody (Western blot). (B) Conversion of Aα and Bβ chains to α and β chains by thrombin treatment in the absence of calcium. (C) Formation of γ dimer (γ-γ) and α polymer (α-poly) upon thrombin treatment in the presence of FXIII and 2 mM calcium was analyzed by SDS-PAGE.

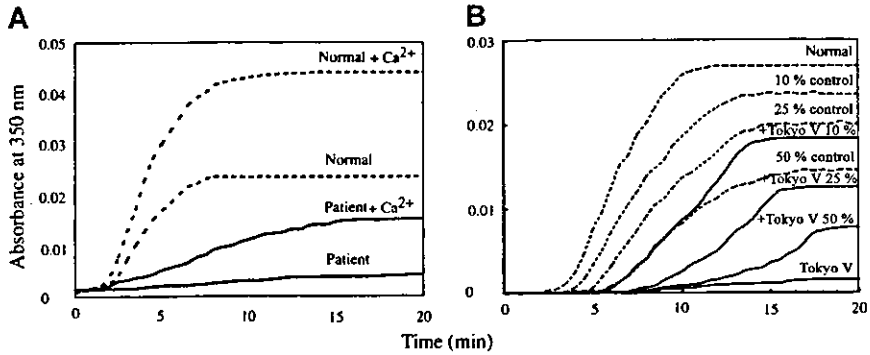

Figure 2. Polymerization profiles of fibrin monomers. (A) Aggregation of fibrin monomers derived from normal fibrinogen (dotted line) or from patient fibrinogen (solid line) at neutral pH in the absence or presence (+Ca^{2+}) of 2 mM calcium was monitored at 350 nm. (B) Aggregation profiles of Tokyo V fibrin monomers (solid line; Tokyo V) and those of normal fibrin monomers in the absence (dotted line; normal) or the presence of increasing concentrations (10%, 25%, and 50%) of Tokyo V fibrin monomers (solid line; +Tokyo V) without calcium are shown. +Tokyo V 10%, +Tokyo V 25%, and +Tokyo V 50% indicate that ratios of amounts of normal fibrin monomers and Tokyo V fibrin monomers are 9:1, 3:1, and 1:1, respectively. The concentration of fibrin monomers (the sum of normal fibrin monomers and Tokyo V fibrin monomers) of each preparation was the same. For the control, aggregation profiles of normal fibrin monomers at reduced concentrations without addition of Tokyo V fibrin monomers are shown as dotted lines.

band on the Western blot, quantified using a densitometer, was approximately 22% of the total amount of the Tokyo V γ chain. In comparison with normal fibrinogen or fibrin, conversion of Tokyo V fibrinogen Aα and Bβ chains to α and β chains by thrombin was similar to normal fibrinogen, as was cross-linking of the γ chain, indicating that release of fibrinopeptides A and B and FXIIIa-mediated γ chain cross-linking of fibrin were not impaired (Figure 1B-C). In contrast, cross-linking of the Tokyo V fibrin α chain was delayed (Figure 1C). Polymerization profiles of fibrin monomers derived from patient fibrinogen were remarkably impaired (Figure 2A). In particular, polymerization of Tokyo V fibrin did not proceed without calcium, confirming that the patient-derived fibrinogen was dysfunctional. Even with 2 mM calcium, absorbance of the Tokyo V fibrin monomer solution increased much slower than the normal fibrin monomer solution, and the maximum absorbance of the Tokyo V fibrin monomer solution was approximately one-third of that of the normal fibrin monomer solution, suggesting that the fibrin polymerization was severely perturbed (Figure 2A). To further study characteristics of Tokyo V fibrin, polymerization of normal fibrin monomers was studied in the presence of increasing concentrations of Tokyo V fibrin monomers. As shown in Figure 2B, polymerization of normal fibrin monomers was inhibited in a dose-dependent manner by the presence of Tokyo V fibrin monomers.

Analysis of soluble Tokyo V fibrin

Tokyo V fibrinogen could be converted to fibrin by thrombin treatment, but its polymerization was severely perturbed, suggesting that Tokyo V fibrin might not form solid clots and might circulate as soluble fibrin. To show that soluble fibrin monomers and polymers were formed upon coagulation and incorporated into clots, normal fibrinogen and Tokyo V fibrinogen were treated with thrombin and FXIII in the presence of calcium and the formed clots were squeezed to separate clots and soluble components. Cross-linked fibrin clots and soluble components were analyzed by SDS-PAGE. The supernatant of a normal fibrin preparation did not contain soluble fibrin even in the presence of EDTA (ethylenediamenetetraacetic acid; Figure 3A). In contrast, a large amount (78.2%) of Tokyo V fibrin remained in the soluble fraction in the presence of EDTA (Figure 3A). Cross-linked soluble Tokyo V fibrin was present in the supernatants of clots formed in the presence of calcium. Analysis of the soluble fraction containing cross-linked soluble fibrin by 3% SDS-PAGE showed that cross-linked soluble Tokyo V fibrin consisted of monomers and a variety of fibrin polymers (Figure 3B). The Western blot analysis of the soluble Tokyo V fibrin showed that the majority of the γ chain was present as the cross-linked γ dimer (γ−γ) but a significant amount of the aberrant γ chain remained as the non–cross-linked form, suggesting that the soluble Tokyo V fibrin monomer consisted of abnormal molecules.

Genetic abnormality of patient fibrinogen genes

We performed genetic analyses of the 3 patient fibrinogen genes as described.[7,9,10] A 5884G>A mutation of the patient fibrinogen γ chain gene was found. The nucleotide mutation was confirmed by 2 independent sequencing methods. As shown in Figure 4, both G and A were found at position 5884 in the directly sequenced PCR-amplified DNA fragments of exon VIII derived from the patient fibrinogen γ chain gene, indicating that the patient had a heterozygous genetic mutation and that this mutation would result in an amino acid substitution of γ Ala327Thr in the affected γ

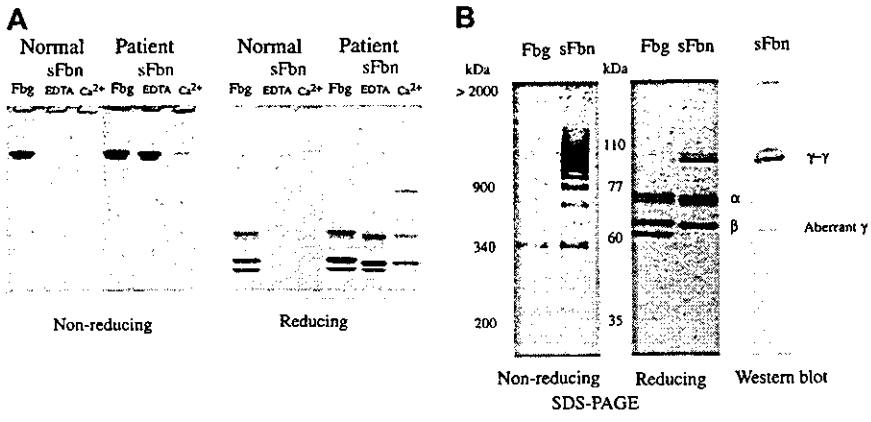

Figure 3. SDS-PAGE analysis of soluble Tokyo V fibrin. Tokyo V fibrinogen was incubated with thrombin (1 U/mL) and FXIII (1 U/mL) in the presence of 2 mM calcium (Ca^{2+}) or 2 mM EDTA (EDTA) at 37°C for 1 hour. Formed clots were squeezed using bamboo sticks to separate soluble fibrin (sFbn) from fibrin clots. (A) Untreated fibrinogen, insoluble clots, and soluble fractions were analyzed by SDS-PAGE using 7.5% polyacrylamide gels under nonreducing and reducing conditions. (B) For analysis of cross-linked soluble Tokyo V fibrin, the supernatant of the patient fibrin preparation was separated on 3% polyacrylamide gels under nonreducing conditions. Fibrinogen (Fbg) was the control. The reduced supernatant sample was analyzed by Western blotting for identification of γ chain. γ-dimers (γ−γ) and the aberrant γ chain (aberrant γ) were indicated.

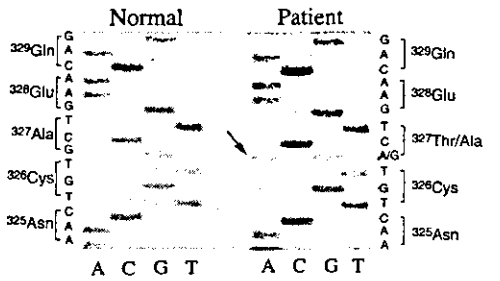

Figure 4. Nucleotide sequences of the γ chain gene exon VIII. Single-stranded DNA, amplified by the asymmetrical PCR method,[7,8] from the γ chain gene exon VIII derived from a healthy subject or the patient, was subjected to direct nucleotide sequencing using ^{35}S-dATP and Sequenase. The pertinent portion of the autoradiography of urea-polyacrylamide gel electrophoresis is shown. Both G and A (arrow) were detected at position 5884 of the patient γ chain gene, coding for Ala (GCT) and Thr (ACT), whereas only G for Ala (GCT) was identified at the same position of the normal γ chain gene.

chain. Based on these data, we performed peptide mapping of lysyl-endopeptidase digests of patient fibrinogen γ chain by high-performance liquid chromatography (HPLC) as described[7-9] and found a small aberrant peptide peak, suggesting that the abnormal γ chain polypeptide was a small part of the purified fibrinogen molecule. N-terminal amino acid sequencing[7-9] of the aberrant peptide found Phe (322), Glu (323), Gly (324), and Thr (327) in the peptide. No Asn was identified in the expected position (325) suggesting that γ Asn325 was glycosylated as a result of the mutation (not shown). The amount of the aberrant peptide was insufficient to confirm the carbohydrate composition linked to the peptide.

Enzymatic removal of N-linked oligosaccharides in fibrinogen

Since there was a higher molecular aberrant γ chain in the Tokyo V fibrinogen preparation, and the presence of an extra oligosaccharide side chain at γ Asn325 of Tokyo V fibrinogen was suggested by the gene analysis and the peptide mapping study, effect of deglycosylation on Tokyo V fibrinogen was studied. As shown in Figure 5, there was the aberrant γ chain in the Tokyo V fibrinogen preparation and this aberrant γ chain band was not detected after N-glycopeptidase F treatment, indicating that the higher molecular aberrant γ chain of Tokyo V fibrinogen migrated to the position similar to the normal γ chain after N-glycopeptidase F treatment. These data strongly suggested the presence of an extra oligosaccharide side chain at γ Asn325 of the abnormal molecule.

Analysis of tPA-catalyzed plasmin digestion of fibrin and tPA-mediated plasmin digestion on fibrin surfaces

Since the amino acid substitution of Tokyo V fibrinogen resided in the γ chain of the D domain, we speculated that binding of tPA to Tokyo V fibrin may be affected. Thus, tPA-catalyzed plasmin digestion of Tokyo V fibrin and tPA-mediated plasmin generation on Tokyo V fibrin surfaces were studied. As shown in Figure 6A, the disappearance of the Tokyo V fibrin α chain was similar to that of normal fibrin, but degradation of the γ chain and β chain was delayed after a 6 hour incubation. This suggested that tPA-dependent fibrinolysis of Tokyo V fibrin was impaired, whereas digestion of Tokyo V fibrin by plasmin without the plasminogen activation process by tPA was virtually the same as that of normal fibrin (not shown). In accordance with these results, tPA-mediated plasmin generation on Tokyo V fibrin surfaces was prolonged compared with that on normal fibrin surfaces (Figure 6B), suggesting that Tokyo V fibrin would be resistant to physiologic fibrinolysis.

Digestion of fibrinogen in the presence of Ca^{2+} ions with plasmin

Since the mutation substituted a Thr at position 327 of the γ chain and possibly added oligosaccharides to Asn325, it may also have affected high-affinity calcium ion binding to the γ chain. Thus, Tokyo V fibrinogen was studied for its resistance to plasmin in the presence of calcium (Figure 7). Normal or Tokyo V fibrinogen was incubated with purified plasmin in the presence of increasing concentrations of calcium and degradation of fibrinogen was analyzed by SDS-PAGE. Normal fibrinogen was converted to the fragment D1 upon incubation with plasmin, but no further degradation of D1 was observed in the presence of 2 mM calcium (Figure 7A). This protection by calcium was observed at low calcium concentration (0.05 mM; Figure 7B). When Tokyo V fibrinogen was incubated with plasmin, fragments D2A and D3 were identified in addition to fragment D1, even at the high calcium concentration (2 mM). The amounts of D2A and D3 were approximately 15% to 20% of the sum of fragments D1, D2A, and D3. These data suggested that the calcium ion–dependent integrity of the Tokyo V fibrinogen conformation was not sufficient to protect the γ chain of fragment D1 from plasmin. The amino acid substitution of Ala to Thr at γ chain 327 and the extra oligosaccharide at Asn325 likely caused structural alternation of the high-affinity calcium binding site in the γ chain. Additionally, approximately 10% to 20% of the purified patient fibrinogen may consist of abnormal molecules because the amount of fragment D1 was not decreased further upon longer incubation.

Scanning electron microscopy of fibrin clots

Scanning electron microscopy was carried out to investigate the structure of Tokyo V fibrin clots. In 2 experiments, a major part of Tokyo V fibrin clots appeared normal at a glance but other parts of Tokyo V fibrin clots looked very loose. That part of Tokyo V fibrin clots was composed of tangled fibers in a variety of diameters, and fibers were highly branched (Figure 8B). Additionally, there were many large pores inside the fibrin networks and many fiber ends were observed. In another scanning electron microscopy experiment, whole Tokyo fibrin clots consisted of very thin and highly branched fibers. There also were large holes in the fibrin networks and many fiber ends were observed at the boundaries (not shown). As described earlier in this paragraph, a variety of fibrin structures were observed in Tokyo V fibrin clots. The presence of fiber ends in the networks may represent early termination of protofibril polymerization. Consistent with the structure of Tokyo V fibrin clots, clottability of Tokyo V fibrin was very low. These findings suggested that Tokyo V fibrin would be fragile.

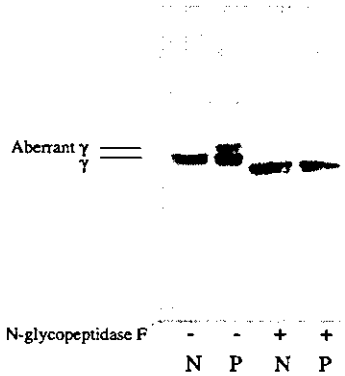

Figure 5. Analyses of deglycosylated fibrinogen. Normal fibrinogen (N) and patient fibrinogen (P) were treated with (+) or without (−) N-glycopeptidase F and analyzed by SDS-PAGE and Western blotting using γ chain–specific monoclonal antibody JIF 25. The γ chain (γ) and the aberrant γ chain (aberrant γ) were indicated.

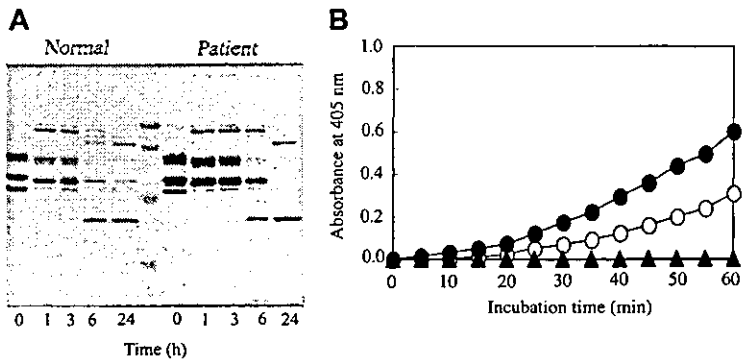

Figure 6. Analysis of tPA-catalyzed plasmin digestion of fibrin and tPA-mediated plasmin generation on fibrin surfaces. (A) Normal or patient fibrinogen was incubated with plasminogen, tPA, FXIII, and thrombin in the presence of calcium. After the indicated time periods, samples were heated at 98°C in the presence of 2% SDS and 10 mM DTT for 5 minutes to terminate the reaction and then analyzed by SDS-PAGE. (B) Normal fibrinogen (●) or patient fibrinogen (○) was incubated with plasminogen, tPA, FXIII, thrombin, and S-2251 in the presence of 2 mM calcium. As a control, normal fibrinogen (▲) was incubated in buffer containing plasminogen, tPA, and S-2251 or in buffer containing plasminogen, tPA, and thrombin. The changes in absorbance at 405 nm were monitored. Background absorbance determined with samples incubated in the absence of S-2251 at 405 nm were subtracted from all values.

Discussion

Fibrinogen Tokyo V has an amino acid substitution in which the γ chain Ala327 is changed to Thr, thereby inserting an N-linked glycosylation consensus sequence and presumably an extra oligosaccharide side chain at γ Asn-325. This mutation is associated with a thrombophilia because fibrinogen Tokyo V was found in a 43-year-old male patient with recurrent thromboembolic episodes, including cerebral infarction at age 36 years, pulmonary embolism at age 42 years, and thrombi in the aorta and the superior mesenteric artery at age 43 years when the patient was admitted to a hospital. Thrombophilic dysfibrinogen is a rare molecular abnormality and mechanisms for thrombophilia may be assigned to defective binding of thrombin to abnormal fibrin, which leads to increased thrombin levels, or to defective stimulatory function of abnormal fibrin in tPA-mediated fibrinolysis.[5]

Data from SDS-PAGE analyses of purified fibrinogen followed by Western blotting using γ chain–specific monoclonal antibody JIF 25, peptide mapping analysis of patient fibrinogen γ chain, and plasmin degradation of the fibrinogen D1 fragment in the presence of calcium suggested that the molecular abnormality of fibrinogen Tokyo V was impaired function and hypofibrinogenemia, even though the patient was heterozygous for the mutation. Although the molecular mechanism for decreased plasma levels of the Tokyo V fibrinogen molecule is not studied yet, a decreased assembly, an intracellular transport defect, or hypercatabolism in the circulation of the abnormal molecules may be responsible for hypodysfibrinogenemia. As reported previously, even a single amino acid substitution can develop an intracellular transport defect of a variety of abnormal molecules including dysfibrinogens.[12,13] Thus, the transport defect of Tokyo V fibrinogen molecules inside the cells would be most likely. Elucidation of the molecular mechanism of hypodysfibrinogenemia of this molecule would be the future study. The genetic analysis indicated the formation of a new N-linked glycosylation consensus sequence in the affected γ chain. Addition of extra oligosaccharides to γ Asn325 was suggested by the amino acid sequence analysis but was not confirmed because of low recovery of the aberrant peptide. Since N-linked glycosylation is a cotranslational event in the endoplasmic reticulum, preceding molecular folding catalyzed by chaperones, Asn325 of the affected γ chain may be glycosylated. We found an aberrant faint polypeptide band, which migrated between the γ chain and the Bβ chain, and the polypeptide was recognized by γ chain–specific monoclonal antibody JIF 25, indicating the presence of a small amount of aberrant γ chain with a higher molecular mass. Analyses of deglycosylated Tokyo V fibrinogen strongly suggested that the aberrant γ chain had an extra oligosaccharide side chain.

The C-terminal region of the γ chain consists of the D domain and has a variety of functional sites including the "a" polymerization pocket for D:E contact, the lateral association site for D:D contact, the tPA binding site, and the high-affinity calcium binding site. The Tokyo V fibrinogen amino acid mutation and the possible presence of oligosaccharide in that region affected these important fibrinogen/fibrin functions directly or indirectly as shown in this study. Based on the crystal structure of the D domain of fibrinogen,[14-17] γ Ala327 resides near the calcium ion binding site and the "a" polymerization pocket. Thus, substitution of γ Ala327Thr

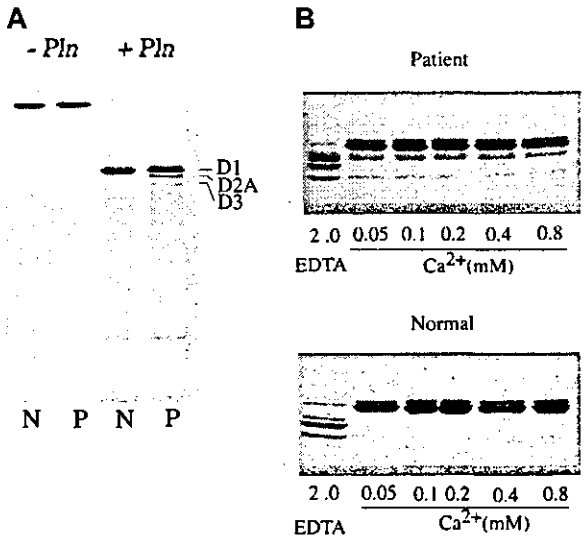

Figure 7. Digestion of fibrinogen in the presence of calcium with plasmin. Fibrinogen (N: normal fibrinogen, P: patient fibrinogen) was treated with plasmin in Tris-buffered saline containing 2 mM calcium (A) or increasing concentrations of calcium or 2 mM EDTA (B) at 37°C for 1 hour. Untreated fibrinogen and plasmin digests of fibrinogen were analyzed by SDS-PAGE under nonreducing conditions. Fragments D1, D2A, and D3 are indicated. The relative amounts of Tokyo V fibrinogen fragments D2A and D3 were quantified by densitometry, and were approximately 17.5% of the sum of fragments D1, D2A, and D3 (mean of 2 experiments).

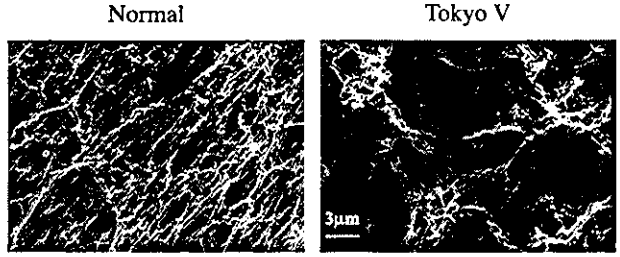

Figure 8. Scanning electron microscopy of fibrin clots. Scanning electron microscopy images of normal fibrin clots (left) and Tokyo V fibrin clots (right) are shown (bar equals 3 μm).

would likely interfere with calcium binding to this region and also affect the polymerization pocket. A new carbohydrate linked to γ Asn325 also would quite likely disrupt the adjacent region, resulting in stronger interference with D-to-E contact than the amino acid substitution of γ Ala327Thr. Since γ Asn325 is off to the side of the buried interface, a γ Asn325–linked carbohydrate may not interfere with the D:D association directly, but may have an indirect influence.

Fibrinogen Tokyo V has the paradoxical feature of decreased functional fibrinogen in the presence of recurrent thrombosis. The polymerization defect of Tokyo V fibrinogen (Figure 2) would account for the decreased fibrinogen level as determined by the thrombin time method (Table 1) and very low clottability (Figure 3). A significant amount of Tokyo V fibrin monomers and polymers remains in the soluble fraction and as these soluble molecules are incorporated into fibrin networks, they may interfere with formation of solid fibrin clots. As evidenced by the scanning electron microscopy analysis showing the loose appearance of and the presence of large pores and many fiber ends in Tokyo V fibrin clots, the structure of Tokyo V fibrin clots may be severely perturbed compared with the normal fibrin clots. Thus, Tokyo V fibrin clots would be fragile, and insoluble fibrin clots may be easily liberated from clots to the circulation. But such Tokyo V fibrin clots also undergo impaired fibrinolysis due to decreased tPA-catalyzed plasmin generation, thereby partly accounting for thrombi formation. Inasmuch as insoluble clots are resistant to fibrinolysis, once insoluble fibrin clots are liberated from thrombi, they may form emboli. The presence of soluble fibrin in the circulation would also contribute to development of a prothrombotic state as well.

Upon conversion of fibrinogen to fibrin, tPA binds to fibrin via Aα and γ chains. Polypeptide segments Aα 148-160[18] and γ 311-336[19] are involved in tPA binding. The amino acid substitution and the presence of possible extra oligosaccharide of Tokyo V fibrinogen/fibrin reside in the proposed tPA binding site in the γ chain, suggesting that tPA binding to the abnormal molecule may be affected directly. A recent report showed that tPA binding segments are buried even in DD fragments, but reversibly expressed on surfaces of DD-E upon association of DD fragments with the E fragments.[20] Thus, severely impaired fibrin polymerization will also influence tPA-mediated plasmin digestion of the mutant fibrin, even though the estimated amounts of abnormal fibrinogen molecules are approximately one-fifth those of normal fibrinogen.

Even with the presence of small amounts of abnormal fibrinogen molecules in the purified material, polymerization of patient fibrin was severely perturbed (Figure 2). During fibrin polymerization, the ratio of abnormal molecule incorporation into polymers could be one-tenth to one-twentieth. Since the molecular abnormality was present in the γ chain that consists of the D domain, expression of the "A" polymerization site in the E domain of the Tokyo V fibrin α chain may not be impaired. Thus, Tokyo V fibrin may have normal "A" knobs in the E domain and dysfunctional "a" polymerization pocket(s) in the D domain(s). Given that the D:E contact would be severely perturbed, extension of protofibrils would be terminated once the abnormal fibrin molecule was associated with normal molecules. If extension of protofibrils does not reach over 600 nm due to incorporation of abnormal molecules, protofibrils may not aggregate to form clots.[21] Inhibition of normal fibrin monomer polymerization by addition of Tokyo V fibrin monomers, the presence of a variety of soluble fibrin polymer species in the supernatant of the patient fibrin preparation, and the presence of fiber ends in fibrin networks support this notion.

In conclusion, fibrinogen Tokyo V is a thrombophilic hypodysfibrinogen with an amino acid substitution of γ Ala327Thr and a possible extra glycosylation at γ Asn325. The thromboembolism may be accounted for by fibrinolysis-resistant fragile clots and formation of a large amount of soluble fibrin caused by conformation defects in the vicinity of the "a" polymerization pocket, the high-affinity calcium ion binding site, and the tPA-binding site of the γ chain.

References

1. Henshen A, Lottspeich F, Kehl M, Southern C. Covalent structure of fibrinogen. Ann N Y Acad Sci. 1983;408:28-43.
2. Doolittle RF. Fibrinogen and fibrin. Annu Rev Biochem. 1984;53:195-299.
3. Huang S, Mulvihill ER, Farrell DH, Davie EW. Biosynthesis of human fibrinogen: subunit interactions and potential intermediates in the assembly. J Biol Chem. 1993;268:8919-8926.
4. Matsuda M. The structure-function relationship of hereditary dysfibrinogens. Int J Hematol. 1996; 64:167-179.
5. Haverkate F, Samama M. Familial dysfibrinogenemia and thrombophilia. Thromb Haemost. 1995; 73:151-161.
6. Brennan SO, Fellowes AP, George PM. Molecular mechanisms of hypo- and afibrinogenemia. Ann N Y Acad Sci. 2001;936:91-100.
7. Mimuro J, Kawata Y, Niwa K, et al. A new type of ser substitution or γArg-275 in fibrinogen Kamogawa I characterized by impaired fibrin assembly. Thromb Haemost. 1999;81:940-944.
8. Yamazumi K, Shimura K, Terukina S, Takahashi N, Matsuda M. A γ methionine-310 to threonine substitution and consequent N-glycosylation at γ asparagine-308 identified in a congenital dysfibrinogenemia associated with posttraumatic bleeding, fibrinogen Asahi. J Clin Invest. 1989;83:1590-1597.
9. Sugo T, Nakamikawa C, Takano H, et al. Fibrinogen Niigata with impaired fibrin assembly: an inherited dysfibrinogen with a Bβ Asn-160 to Ser substitution associated with extra glycosylation at Bβ Asn-158. Blood. 1999;94:3806-3813.
10. Mimuro J, Hamano A, Tanaka T, et al. Hypofibrinogenemia caused by a nonsense mutation in the fibrinogen Bβ chain gene. J Thromb Haemost. 2003;1:2356-2359.
11. Naito M, Mimuro J, Endo H, et al. Defective sorting to secretory vesicles in the trans Golgi network is partly responsible for protein C deficiency: molecular mechanisms of impaired secretion of abnormal protein C R169W, R352W, and G376D. Circ Res. 2003;92:865-872.
12. Terasawa F, Okumura N, Kitano K, et al. Hypofibrinogenemia associated with a heterozygous missense mutation 153Cys to Arg (Matsumoto IV): in vitro expression demonstrates defective secretion of the variant fibrinogen. Blood. 1999; 94:4122-4131.
13. Brennan SO, Wyatt J, Medicina D, Callea F, George PM. Fibrinogen Brescia: hepatic endoplasmic reticulum storage and hypofibrinogenemia because of a γ284 Gly → Arg mutation. Am J Pathol. 2000;157:189-196.
14. Spraggon G, Everse SJ, Doolittle RF. Crystal structure of fragment D from human fibrinogen and its crosslinked counterpart from fibrin. Nature. 1997;389:455-462.
15. Pratt KP, Cote HCF, Chung DW, Stenkamp RE, Davie EW. The primary fibrin polymerization pocket: three-dimensional structure of a 30-kDA C-terminal γ chain fragment complexed with the peptide Gly-Pro-Arg-Pro. Proc Natl Acad Sci U S A. 1997;94:7176-7181.
16. Cote HC, Lord ST, Pratt KP. γ-chain dysfibrinogenemia: molecular structure-function relationships of naturally occurring mutations in the chain γ of human fibrinogen. Blood. 1998;92:2195-2212.
17. Cote HC, Pratt KP, Davie EW, Chung DW. The polymerization pocket "a" with carboxyl-terminal region of the γ chain of human fibriogen is adjacent to but independent from the calcium-binding site. J Biol Chem. 1997;272:23792-23798.
18. Nieuwenhuizen W, Vermond A, Voskuilen M, Traas DW, Verheijen JH. Identification of a site in fibrin(ogen) which is involved in the acceleration of plasminogen activation by tissue-type plasminogen activator. Biochim Biophys Acta. 1983;748: 86-92.
19. Yonekawa O, Voskuilen M, Nieuwenhuizen W. Localization in the fibrinogen γ chain of a new site that is involved in the acceleration of by tissue-type plasminogen activator catalyzed activation of plasminogen. Biochem J. 1992; 283:187-191.
20. Yakovlev S, Makogonenko E, Kurochkina N, Nieuwenhuizen, Ingham K, Medved L. Conversion of fibrinogen to fibrin: mechanism of exposure of tPA- and plasminogen-binding sites. Biochemistry. 2000;39:15730-15741.
21. Hantgan R, McDonagh J, Hermans J. Fibrin assembly. Ann N Y Acad Sci. 1983;408:344-366.

Journal of General Virology (2004), 85, 2209–2214 DOI 10.1099/vir.0.79940-0

Short Communication

The adenovirus E1A and E1B19K genes provide a helper function for transfection-based adeno-associated virus vector production

Takashi Matsushita,[1] Takashi Okada,[1] Toshiya Inaba,[2] Hiroaki Mizukami,[1] Keiya Ozawa[1] and Peter Colosi[3]

Correspondence
Takashi Okada
tokada@jichi.ac.jp
Peter Colosi
PColosi@avigen.com

[1]Division of Genetic Therapeutics, Center for Molecular Medicine, Jichi Medical School, 3311-1 Yakushiji, Minami-kawachi, Kawachi, Tochigi 329-0489, Japan

[2]Department of Molecular Oncology, Research Institute for Radiation Biology and Medicine, Hiroshima University, Hiroshima 734-8553, Japan

[3]Avigen Inc., Alameda, CA, USA

Received 26 December 2003
Accepted 17 May 2004

Although the adenoviral E1, E2A, E4 and VA RNA regions are required for efficient adeno-associated virus (AAV) vector production, the role that the individual E1 genes (*E1A*, *E1B19K*, *E1B55K* and *protein IX*) play in AAV vector production has not been clearly determined. E1 mutants were analysed for their ability to mediate AAV vector production in HeLa or KB cells, when cotransfected with plasmids encoding all other packaging functions. Disruption of *E1A* and *E1B19K* genes resulted in vector yield reduction by up to 10- and 100-fold, respectively, relative to the wild-type E1. Interruption of the *E1B55K* and *protein IX* genes had a modest effect on vector production. Interestingly, expression of anti-apoptotic E1B19K cellular homologues such as Bcl-2 or Bcl-x_L fully complemented E1B19K mutants for AAV vector production. These findings may be valuable for the future development of packaging cell lines for AAV vector production.

Adeno-associated virus (AAV)-based vector systems are particularly attractive vehicles for clinical applications requiring long-term *in vivo* gene expression from post-mitotic tissues. AAV vectors have been shown to promote stable expression of a wide variety of transgenes in numerous tissues, including skeletal and cardiac muscle, liver, the central nervous system and retina (Rabinowitz & Samulski, 1998). Overt evidence of inflammation is either minimal or non-existent in target tissues immediately following AAV vector administration. Furthermore, cytotoxic T-lymphocyte responses are not normally elicited to transgene products delivered by AAV vectors, even when such proteins are foreign to the host (Jooss *et al.*, 1998). AAV vectors are considered to be relatively safe because the parental virus is non-pathogenic and unable to replicate in the absence of a co-infecting helper virus. Additionally, current production methods have reduced the regeneration of replication competent wild-type AAV during vector production to undetectable levels (Allen *et al.*, 1997). Finally, the robust protein capsid of AAV makes AAV vectors particularly amenable to existing production methods for protein pharmaceuticals (Gao *et al.*, 2000) and confers upon them desirable drug stability characteristics.

AAV2, the parent virus from which the vector system is derived, is replication defective and requires co-infection of helper viruses to propagate. Adenovirus (Atchinson *et al.*, 1965) and herpes virus (Buller *et al.*, 1981) act as complete helpers and vaccinia virus (Schlehofer *et al.*, 1986) acts as a partial helper. The set of adenoviral (type 2 or 5) genes that facilitate AAV2 propagation has been defined and consists of E1A, E1B55K, the VA RNAs, E2A and E4orf6 (Samulski & Shenk, 1988). E1A acts as a cue to begin virus replication by up-regulating transcription from the *rep* gene promoters, P5 and P19 (Tratschin *et al.*, 1984) and by activating the early adenovirus promoters. E1A is also required to drive the host cell into the S-phase of the cell cycle for viral DNA replication because the AAV encoded proteins are not capable of this function. An adverse effect of E1A is that it stabilizes p53, which leads to apoptosis (Lowe *et al.*, 1993). To prevent this, the E1B55K and the E4orf6 proteins form a complex with p53 and cause it to be degraded through ubiquitin-mediated proteolysis (Querido *et al.*, 1997; Steegenga *et al.*, 1998). Later in infection, E1B55K and E4orf6 form a heterodimer that causes the preferential export of AAV and adenoviral late mRNAs from the nucleus while inhibiting the transit of adenoviral early and cellular mRNAs (Pilder *et al.*, 1986). The 72 kDa DNA-binding protein encoded by E2A has functions in viral DNA replication, viral mRNA processing and export, and AAV promoter regulation (Carter *et al.*, 1992; Ward *et al.*, 1998; Chang & Shenk, 1990). It causes an increase in the intracellular levels of the

single- and double-stranded forms of the AAV genome, the spliced forms of the rep proteins, and dramatically increases capsid protein production. Lastly, the VA RNAs inhibit the interferon-inducible eIF-2 protein kinase, thereby circumventing this cellular anti-viral mechanism from blocking viral protein translation (West *et al.*, 1987).

With respect to E2A, E4orf6 and the VA RNAs, the helper gene requirement for AAV vector and virus production is identical. We and others, have shown that plasmids encoding these genes, when cotransfected into 293 cells along with plasmids encoding rep/cap and a vector, mediate higher levels of vector production than that produced by adenovirus infection (Xiao *et al.*, 1998; Matsushita *et al.*, 1998). This so-called 'triple plasmid' transfection method forms the basis of the current scale-up vector production effort at Avigen and has a respectable mean production efficiency of 1×10^{13} vector genomes produced per 850 cm^2 roller bottle. A report was published describing a method for producing AAV vector in 293 cells using only E4orf6 as the helper gene (Allen *et al.*, 2000). This method requires the use of a heterologous promoter to drive the capsid gene and is about 10-fold less productive than methods using a plasmid encoding all three adenoviral helper genes (unpublished data).

The genes of the E1 region have not been analysed for their contribution to AAV vector production. In this study, we have investigated the role of the *E1A* and *E1B* genes in AAV vector production by using a series of E1 mutant plasmids and cell lines that lack adenoviral genes. E1A was required for efficient vector production. In contrast to the helper requirements for AAV production, our data indicated that *E1B19K* gene greatly augmented vector production, however, *E1B55K* gene did not.

The contributions of each of the component genes from the E1 region to AAV helper function was assessed by creating a set of plasmids with mutations in the *E1A*, *E1B19K*, *E1B55K* or *protein IX* genes and then testing them for their ability to support transfection-based AAV vector production. At least one truncation or one deletion mutation was made for each gene (Fig. 1).

For vector construction the plasmid pE1, which encodes the *E1A*, *E1B19K*, *E1B55K* and *protein IX* genes, was created from Ad2 DNA (Invitrogen). Briefly, the *Afl*III fragment (nt positions 142–5927) of Ad2 was cloned into the *Afl*III site of pBR322 (New England Biolabs) to generate pE1. pE1A-825stop was constructed by the insertion of an adapter (CCGGACTAATTAACTAGT), which includes a stop codon and an *Spe*I site, into the *Bsp*EI site of pE1. Similarly, pE1B19K-1912stop, pE1B55K-2243stop,

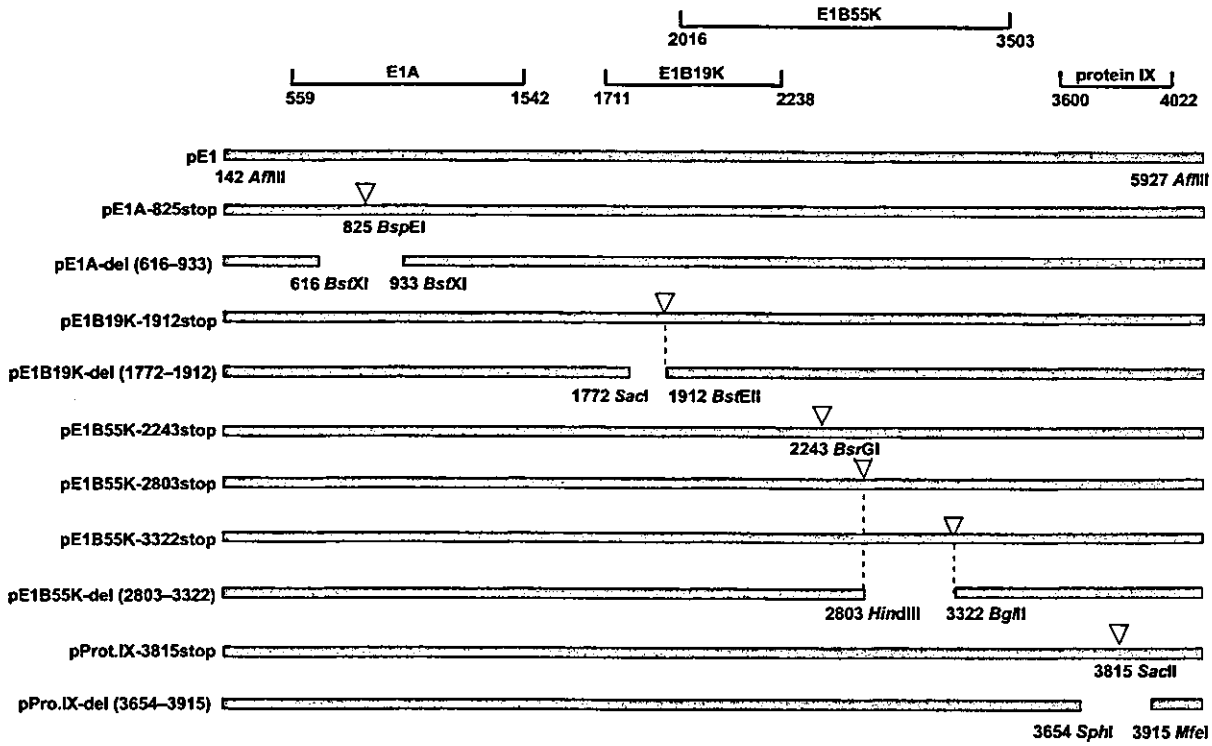

Fig. 1. Schematic representation of plasmids harbouring adenoviral E1 mutants used in this study. A 5·8 kb DNA fragment of adenovirus type 2 was cloned into the *Afl*III site of pBR322. pE1 encodes the entire E1 region, and the E1 mutant plasmids shown here were derived from it. The vertical flags mark the positions of inserted stop codons. The gaps in pE1A, pE1B19K, pE1B55K or pProt.IX constructs represent deletions.

pE1B55K-2803stop and pE1B55K-3322stop were made by the insertion of oligonucleotides into the *Bst*EII, *Bsr*GI, *Hin*dIII and *Bgl*II sites of pE1, respectively. pE1A-del (616–933) has a deletion of a 318 bp segment (positions 616–933 in Ad2). pE1B19K-del (1772–1912) and pE1B55K-del (2803–3322) have the same deletions as *dl337* (Pilder *et al.*, 1984) and *dl338* (Pilder *et al.*, 1986), respectively, used by Samulski & Shenk (1988) to examine E1 helper function for AAV2 production. Briefly, pE1B19K-del (1772–1912) lacks sequences between positions 1772 and 1912, and pE1B55K-del (2803–3322) lacks sequences between positions 2803 and 3322. pProt.IX-3815stop was constructed by the insertion of oligonucleotides into a *Sac*II site. pProt.IX-del (3654–3915) lacks a 262 bp segment (between positions 3654 and 3915 of Ad2).

The helper activities of the various E1 plasmids were assayed by cotransfecting them with a plasmid encoding both an AAV CMV*lacZ* vector and rep/cap (pW4389LacZ), and a plasmid encoding the adenovirus-2 VA RNA, E2A and E4 regions (Pladeno5), into KB or HeLa cells, and then quantifying *lacZ* vector production as described previously (Matsushita *et al.*, 1998). AAV vector was harvested 40 or 72 h after transfection and stocks were prepared by the freeze-thaw method. AAV vector production was quantified by titration of the vector stocks in 293 cells in the presence of adenovirus, followed by X-Gal staining and manual counting by light microscopy. For each experiment, all constructs were tested using triplicate production cultures, and all experiments were conducted at least three times, independently.

Elimination of the entire E1 region resulted in 2 (HeLa cells) to 3 log (KB cells) reduction in vector production relative to production in the presence of pE1, a plasmid encoding the entire E1 region ($P<0{\cdot}01$ by Student's *t*-test) (Fig. 2a, b). Disruption of the *E1A* genes, whether by truncation or deletion, caused 1 (HeLa cells) to 1·5 log (KB cells) reduction in vector production ($P<0{\cdot}01$). Truncations or deletions in the *E1B19K* gene also resulted in substantial reduction in vector production, 1 log in HeLa cells and greater than 2 logs in KB cells ($P<0{\cdot}01$). The lesser severity of the E1B19K mutant in HeLa cells, relative to KB cells, may be due to the relatively high level of Bcl-2 expression in HeLa cells (Liang *et al.*, 1995), or the human papilloma virus E6/E7 genes they harbour. The E6/E7 genes have been shown to facilitate some of the processes in AAV replication (Walz *et al.*, 1997). In most cases, disruption of the *E1B55K* and *protein IX* genes had a modest effect on vector production in either HeLa or KB cells. Two constructs, pE1B55K-2243stop and pProt.IX-3815stop showed fivefold reduction in vector yield in KB cells but little reduction in HeLa cells.

Our results differ substantially from those of Samulski & Shenk (1988) who examined the effect of E1B adenovirus mutants on AAV2 production, DNA replication, and mRNA and protein expression. This group found that an E1B19K adenovirus-2 mutant (*dl337*) mediated efficient AAV production from HeLa cells transfected with a plasmid encoding an AAV wild-type provirus (pSM620) but that

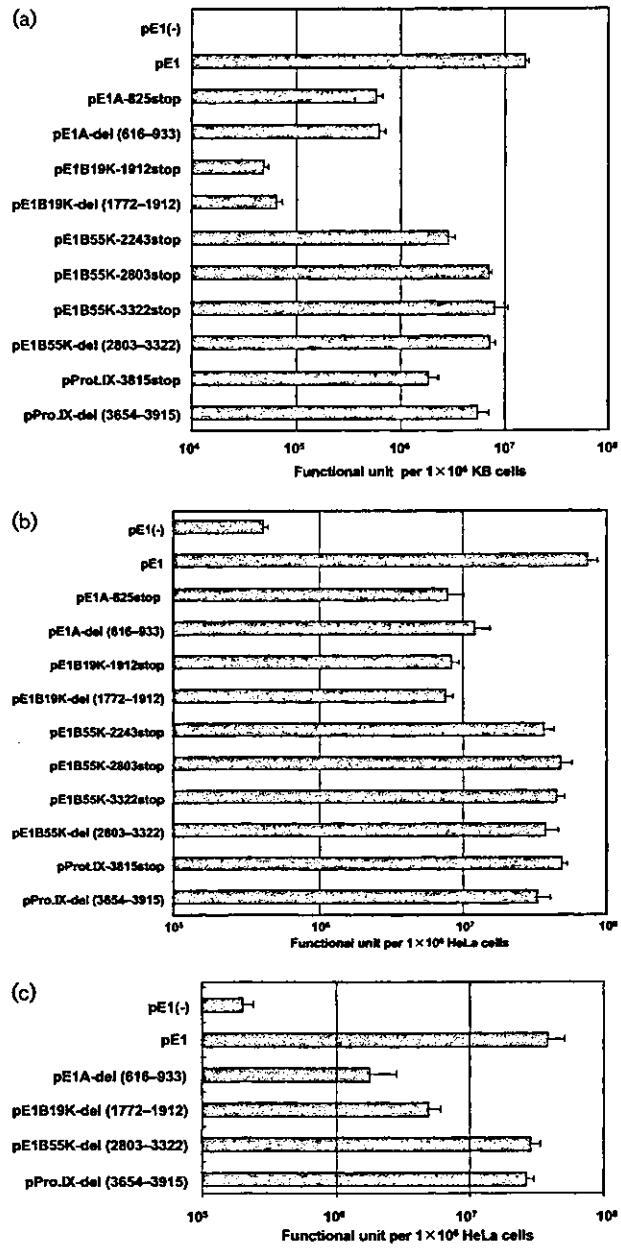

Fig. 2. Comparison of E1 mutant plasmids with respect to AAV helper function in KB (a) and HeLa cells (b) at 72 h after transfection, or in HeLa cells (c) at 40 h after the transfection. AAV *lacZ* vector was produced by the transfection of HeLa or KB cells with pW4389lacZ (encodes rep/cap and an AAV *lacZ* vector) and pladeno 5 (encodes the E2A, E4 and VA RNA regions), in the presence and absence of the indicated E1 plasmids. AAV vector production was assessed by titration of *lacZ* vector in 293 cells. pE1 (-) is identical to pBR322 without the expression cassette. Each bar represents the mean value obtained from triplicate cultures, and the error bar represents the standard deviation.

E1B55K (*dl338*) and E4orf6 (*dl355*) adenovirus mutants did not. AAV virion production was measured at a 40 h time point. The E1B55K and E4orf6 defects were caused by a delay in AAV mRNA accumulation that resulted in delays in viral DNA replication, capsid expression and ultimately virus production. AAV mRNA, DNA and capsid protein concentrations in cultures infected with E1B55K and E4orf6 mutants eventually reached levels seen in cultures infected by wild-type adenovirus but at longer time points, 72–96 h for adenovirus mutants compared with 24–40 h for wild-type adenovirus.

An important difference between our study and that of Samulski & Shenk (1988) was the timing of AAV/AAV vector harvest, 40 h in our study versus 72 h in theirs. Therefore, we examined a subset of the E1 region plasmids in transfection experiments using the same 40 h time point for vector harvest (Fig. 2c). The results were essentially similar to those at the 72 h time point and still differed from those produced by the adenovirus mutants. This observed difference in helper gene requirement may be attributable to technical factors associated with using virus infection or DNA transfection. A possible explanation for the conclusions reached by Samulski & Shenk (1988) might be the differences in the growth rates of the adenovirus mutants tested. The E1B55k mutant, *dl338*, was reported to grow inefficiently (100-fold reduced relative to wild-type) in HeLa cells (Pilder *et al.*, 1986) while the E1B19K mutant, *dl337*, was reported to be less defective (about 10-fold reduced relative to wild-type) (Pilder *et al.*, 1984). The lag in AAV mRNA, DNA and virus production seen with the E1B55K mutant may be simply because of a slow growing helper virus, resulting in low copy numbers of all of the adenovirus helper genes, and may not be directly due to the lack of the mutated gene. The observation that E1B19K is apparently not required for adenovirus mediated AAV production is harder to explain. It is tempting to speculate that the transfection-based production system benefits from additional anti-apoptitic activity provided by E1B19K. If this is true, this requirement does not appear to be cell-type or transfection-reagent specific (calcium phosphate and polycation-based transfection reagents both show an E1B19K effect, data not shown), and may have something to do with the adenoviral helper gene dose or kinetics of expression. Other differences between the two methods of identifying AAV helper function include: transfection method, the packaging of AAV virus versus a vector, and the use of replicating helper (AAV) versus non-replicating plasmid helpers. Full resolution of these issues will require further experimentation.

The adenovirus *E1B19K* gene, and its cellular homologues Bcl-2 and Bcl-x_L, encode anti-apoptotic proteins that function by inhibiting proapoptotic Bcl-2 homologues, such as Bax and Bak, by forming inactive heterodimers with them. To determine whether other anti-apoptotic members of the Bcl-2 family could augment AAV vector production, plasmid vectors expressing the *E1B19K*, *Bcl-2* or *Bcl-x_L* gene

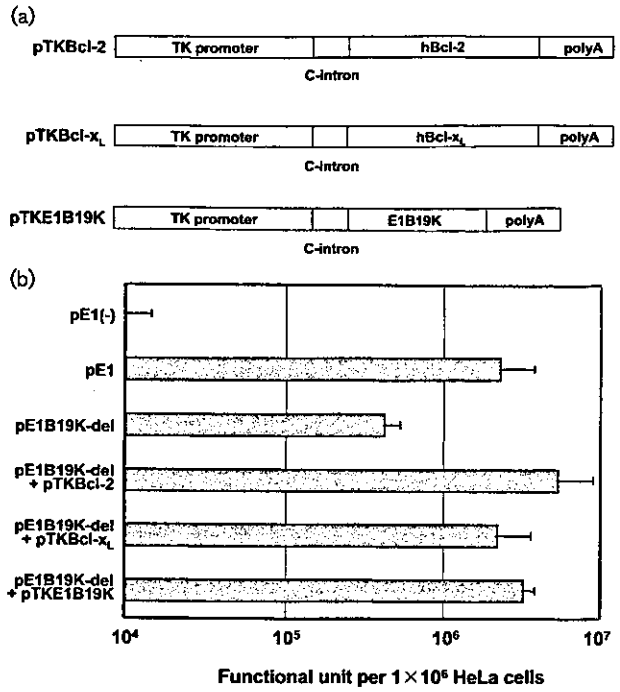

Fig. 3. (a) Schematic representation of Bcl-2, Bcl-x_L and E1B19K expression plasmids. TK promoter, HSV-*tk* promoter; C-intron, chimeric CMV/β-globin intron; polyA, SV40 late polyadenylation signal; hBcl-2, human Bcl-2 cDNA; hBcl-x_L, human Bcl-x_L cDNA; and E1B19K, adenovirus type 2 early region 1B 19 kDa protein gene. (b) Bcl-2 family members complement the vector production defect of an E1B19K mutant in HeLa cells. AAV *lacZ* vector was produced by the transfection of HeLa cells with pW4389lacZ (encodes rep/cap and an AAV *lacZ* vector), pladeno 5 (encodes the E2A, E4 and VA RNA regions), and pE1B19K-del (1772–1912), in the presence and absence of the indicated plasmids expressing Bcl-2 family genes, including E1B19K. AAV vector production was assessed by titration of *lacZ* vector in 293 cells. Each bar represents the mean value of triplicate cultures and the error bar represents the standard deviation.

products were tested for their ability to complement the vector production defect of the E1B19K deletion mutant, pE1B19K-del (1772–1912) (Fig. 3a). pTKPRMCS was assembled by the removal of a *Renilla* luciferase (*Rluc*) reporter gene from pRL-TK (Promega) (between the *Nhe*I and *Xba*I sites) and insertion of a multiple cloning site (between the *Kpn*I and *Xba*I sites) from pBluescript II (Stratagene). pTK-Bcl-2 and pTK-Bcl-x_L were created by the insertion of human Bcl-2 and Bcl-x_L cDNA sequences, respectively, into pTKPRMCS. pTK-E1B19K was constructed by the insertion of the E1B19K fragment into pTKPRMCS. As shown in Fig. 3(b), plasmids expressing E1B19K, Bcl-2 or Bcl-x_L restored vector production of the E1B19K deletion mutant to levels equivalent to that produced by the wild-type pE1 plasmid. The use of the medium strength HSV-*tk* promoter to drive the expression

of the Bcl-2 homologues was essential for helper function. CMV-driven constructs produced low vector yields in a dominant fashion and caused a substantial increase in apoptosis (data not shown).

The fact that E1B19K mutants can be complemented by similarly anti-apoptotic cellular homologues such as Bcl-2 or Bcl-x_L suggests a common mechanism, the inhibition of Bak/Bax-mediated apoptosis. Interestingly, no increase in DNA ladder formation is seen in HeLa cells when transfected with E1B19K mutant plasmids relative to wild-type plasmids (data not shown). Consequently, the mechanism of vector production augmentation is not clear.

Current transfection-based AAV vector production methods are sufficient to commercially support gene therapy applications with large doses and small patient populations (e.g. haemophilia, other genetic diseases) or applications with small doses and large patient populations (e.g. Parkinson's disease). Applications with large doses and large patient populations (e.g. heart failure) will be a challenge for transfection-based production methods that scale linearly. Consequently, the construction of a producer cell line that is both helper virus-free, and suspension culture-adaptable, is of great interest. This is a formidable task since many of the viral helper proteins are toxic to the cell either alone (e.g. E2A) or in combination with other helper functions (e.g. E4orf6 and E1B55K, E1A and *rep*). The task is further complicated by genes such as E1B19K that must be expressed in a rather precise manner. Packaging cell lines containing inducible E1 genes, along with the E2a, VA and E4 regions, and an integrated AAV vector have been produced but were found to suffer from relatively low vector yield and substantial production instability (Qiao *et al.*, 2002). Both of these problems were likely due to, or exacerbated by, helper gene toxicity. Our data indicates that one source of toxicity, the inhibition of host mRNA nuclear export mediated by the E4orf6/E1B55K heterodimer, could be eliminated by not including the E1B55K gene in packaging cell lines.

Defining the minimum set of helper genes necessary for efficient vector production is the first step in creating suitable packaging cell lines for AAV vectors. Using our transfection-based assay, we define that set to be E1A, E1B19K, the VA RNAs, E2A and E4orf6 genes.

Acknowledgements

We thank Dr Lawrence H. Boise for providing the Bcl-x_L cDNA, and Dr Michael Lochrie and Dr Matthew Weitzman for manuscript review and helpful comments. We also thank Dr Tatsuya Nomoto and Ms Miyoko Mitsu for their encouragement and support. This work was supported in part by a Grant-in-Aid for Scientific Research on Priority Areas from the Ministry of Education, Science, Sports and Culture of Japan; a grant for Research on Human Genome and Gene Therapy from the Ministry of Health, Labour and Welfare of Japan; Core Research for Evolutional Science and Technology (CREST) of the Japan Science and Technology Corporation (JST); and a Jichi Medical School young investigator award.

References

Allen, J. M., Debelak, D. J., Reynolds, T. C. & Miller, A. D. (1997). Identification and elimination of replication-competent adeno-associated virus (AAV) that can arise by nonhomologous recombination during AAV vector production. *J Virol* **71**, 6816–6822.

Allen, J. M., Halbert, C. L. & Miller, A. D. (2000). Improved adeno-associated virus vector production with transfection of a single helper adenovirus gene, E4orf6. *Mol Ther* **1**, 88–95.

Atchinson, R. W., Casto, B. C. & Hammon, W. M. (1965). Adenovirus-associated defective virus particles. *Science* **149**, 754–756.

Buller, R. M., Janik, J. E., Sebring, E. D. & Rose, J. A. (1981). Herpes simplex virus types 1 and 2 completely help adenovirus-associated virus replication. *J Virol* **40**, 241–247.

Carter, B. J., Antoni, B. A. & Klessig, D. F. (1992). Adenovirus containing a deletion of the early region 2A gene allows growth of adeno-associated virus with decreased efficiency. *Virology* **191**, 473–476.

Chang, L. S. & Shenk, T. (1990). The adenovirus DNA-binding protein stimulates the rate of transcription directed by adenovirus and adeno-associated virus promoters. *J Virol* **64**, 2103–2109.

Gao, G., Qu, G., Burnham, M. S. & 7 other authors (2000). Purification of recombinant adeno-associated virus vectors by column chromatography and its performance *in vivo*. *Hum Gene Ther* **11**, 2079–2091.

Jooss, K., Yang, Y., Fisher, K. J. & Wilson, J. M. (1998). Transduction of dendritic cells by DNA viral vectors directs the immune response to transgene products in muscle fibers. *J Virol* **72**, 4212–4223.

Liang, X. H., Mungal, S., Ayscue, A., Meissner, J. D., Wodnicki, P., Hockenbery, D., Lockett, S. & Herman, B. (1995). Bcl-2 proto-oncogene expression in cervical carcinoma cell lines containing inactive p53. *J Cell Biochem* **57**, 509–521.

Lowe, S. W., Ruley, H. E., Jacks, T. & Housman, D. E. (1993). p53-dependent apoptosis modulates the cytotoxicity of anticancer agents. *Cell* **74**, 957–967.

Matsushita, T., Elliger, S., Elliger, C., Podsakoff, G., Villarreal, L., Kurtzman, G. J., Iwaki, Y. & Colosi, P. (1998). Adeno-associated virus vectors can be efficiently produced without helper virus. *Gene Ther* **5**, 938–945.

Pilder, S., Logan, J. & Shenk, T. (1984). Deletion of the gene encoding the adenovirus 5 early region 1b 21,000-molecular-weight polypeptide leads to degradation of viral and host cell DNA. *J Virol* **52**, 664–671.

Pilder, S., Moore, M., Logan, J. & Shenk, T. (1986). The adenovirus E1B-55K transforming polypeptide modulates transport or cytoplasmic stabilization of viral and host cell mRNAs. *Mol Cell Biol* **6**, 470–476.

Qiao, C., Li, J., Skold, A., Zhang, X. & Xiao, X. (2002). Feasibility of generating adeno-associated virus packaging cell lines containing inducible adenovirus genes. *J Virol* **76**, 1904–1913.

Querido, E., Marcellus, R. C., Lai, A., Charbonneau, R., Teodoro, J. G., Ketner, G. & Branton, P. E. (1997). Regulation of p53 levels by the E1B 55-kilodalton protein and E4orf6 in adenovirus-infected cells. *J Virol* **71**, 3788–3798.

Rabinowitz, J. E. & Samulski, J. (1998). Adeno-associated virus expression systems for gene transfer. *Curr Opin Biotechnol* **9**, 470–475.

Samulski, R. J. & Shenk, T. (1988). Adenovirus E1B 55-Mr polypeptide facilitates timely cytoplasmic accumulation of adeno-associated virus mRNAs. *J Virol* **62**, 206–210.

Schlehofer, J. R., Ehrbar, M. & zur Hausen, H. (1986). Vaccinia virus, herpes simplex virus, and carcinogens induce DNA amplification in a human cell line and support replication of a helpervirus dependent parvovirus. *Virology* **152**, 110–117.

Steegenga, W. T., Riteco, N., Jochemsen, A. G., Fallaux, F. J. & Bos, J. L. (1998). The large E1B protein together with the E4orf6 protein

target p53 for active degradation in adenovirus infected cells. *Oncogene* **16**, 349–357.

Tratschin, J. D., West, M. H., Sandbank, T. & Carter, B. J. (1984). A human parvovirus, adeno-associated virus, as a eucaryotic vector: transient expression and encapsidation of the procaryotic gene for chloramphenicol acetyltransferase. *Mol Cell Biol* **4**, 2072–2081.

Walz, C., Deprez, A., Dupressoir, T., Durst, M., Rabreau, M. & Schlehofer, J. R. (1997). Interaction of human papillomavirus type 16 and adeno-associated virus type 2 co-infecting human cervical epithelium. *J Gen Virol* **78**, 1441–1452.

Ward, P., Dean, F. B., O'Donnell, M. E. & Berns, K. I. (1998). Role of the adenovirus DNA-binding protein in *in vitro* adeno-associated virus DNA replication. *J Virol* **72**, 420–427.

West, M. H., Trempe, J. P., Tratschin, J. D. & Carter, B. J. (1987). Gene expression in adeno-associated virus vectors: the effects of chimeric mRNA structure, helper virus, and adenovirus VA1 RNA. *Virology* **160**, 38–47.

Xiao, X., Li, J. & Samulski, R. J. (1998). Production of high-titer recombinant adeno-associated virus vectors in the absence of helper adenovirus. *J Virol* **72**, 2224–2232.

RESEARCH

Separate Control of Rep and Cap Expression Using Mutant and Wild-Type LoxP Sequences and Improved Packaging System for Adeno-Associated Virus Vector Production

*Hiroaki Mizukami, Takashi Okada, Yoji Ogasawara, Takashi Matsushita, Masashi Urabe, Akihiro Kume, and Keiya Ozawa**

Abstract

Adeno-associated virus (AAV) vectors are a practical choice for gene transfer, and demand for them is increasing. To cope with the necessity in the near future, we have developed a number of approaches to establish packaging cell lines for the production of AAV vectors. In our previous study, a highly regulated expression of large Rep proteins was obtained by using the Cre–loxP switching system. Therefore, in the present study, to regulate Cap expression as well, we developed an inducible expression system for both Rep and Cap proteins by using an additional set of mutant loxP sequences. The mutants possess two base alterations in the spacer region of loxP and recombine specifically with the same counterpart in the presence of Cre. By using two separate plasmids, one with mutant and the other with wild-type loxP sequences, the expression of two different proteins can be induced simultaneously by Cre recombinase. When the LacZ-encoding plasmid vector was used as a packaging model, a significant packaging titer of 2.1×10^{10} genome copies per 10-cm dish was obtained. These results indicate the importance of controlling Cap expression, in addition to Rep, to achieve an optimum production rate for AAV vectors.

Index Entries: Cre–loxP; mutant loxP; dependovirus; AAV vector; packaging cell line; 293 cells.

1. Introduction

Adeno-associated viruses (AAVs) are currently being investigated as a gene transfer vector for a variety of applications. Several diseases are thought to be prime candidates for AAV vector-medicated therapeutic intervention; clinical trials are already set out for the correction of hemophilia B *(1)*, and for Parkinson's disease in the near future *(2,3)*. However, one drawback to the use of AAV is difficulty in making large-scale preparations. To improve the process of preparation, we have developed packaging cell lines for AAV *(4,5)*. Early studies indicate that in addition to Rep, relatively large amounts of Cap proteins should be expressed to achieve a high titer of virus production, despite the fact that constitutive expression of these proteins has cytotoxic consequences *(6,7)*. Therefore, controlling the expression profiles for these proteins has vital significance. For this purpose, the Cre–loxP system is one of the best-known approaches as an induction system, and in our previous study we used loxP sequences to regulate Rep expression *(4)*. However, there was a limitation to this approach in that Cap expression could not be regulated efficiently; only Rep expression could be regulated. To control Cap expression in addition to Rep expression, we used mutant loxP sequences along with the wild type. These mutant loxP sequences are shown to recombine specifically with each

*Author to whom all correspondence and reprint requests should be addressed: Dr. Keiya Ozawa, Division of Genetic Therapeutics, Center for Molecular Medicine, Jichi Medical School, 3311-1, Yakushiji, Minamikawachi-machi, Kawachi-gun, Tochigi, 329-0498, Japan.E-mail: kozawa@ms2.jichi.ac.jp

other, but less efficiently with wild-type sequences on treatment with Cre *(8)*. In the present study, we compared the efficiency of recombination and designed plasmids to express optimal amounts of Rep and Cap proteins on Cre treatment. By optimizing these parameters, we developed a packaging cell line with improved production rate compared with our prototype cell line.

2. Materials and Methods

2.1. Cells and Plasmids

A human embryonic kidney cell line, known as 293 cells *(9)*, was maintained as described previously *(4)*. Plasmid ploxlox (a gift from Dr. Jamey D. Marth), which contains two adjacent loxP sequences in the same direction, was used as a backbone for the wild-type loxP *(10)*. To make plas-mids with mutant loxP, the sequences corresponding to the spacer region of loxP were mutated by synthesizing oligonucleotides based on published sequence information (**Fig. 1A**) *(8)*. Briefly, the spacer region of wild-type loxP constitutes ATGTATGC; for the loxP (V) and loxP(S), the sequences correspond to 5'-ATGT GTAC-3' and 5'-AAGTATCC-3', respectively. The CAG promoter (a gift from Dr. J Miyazaki, Osaka University, Japan) *(11)*, neomycin resistance gene, blasticidin S resistance gene (Invitrogen Corp., Carlsbad, CA), bacterial LacZ sequence, and AAV sequences corresponding to *p5*, *rep*, and *cap* genes were excised and ligated to complete plasmids named CAPBPL, CAVBVL, CASBSL, CAPBPC, and p5SNSR, respectively (*see* **Fig. 1B**), using standard techniques as reported previously *(4)*.

2.2. Induction of Recombination and Demonstration of Gene Expression

Plasmids encoding *LacZ* gene with the "stuffer" sequences between the two loxP sequences (CAPBPL, CAVBVL, CASBSL) were introduced into 293 cells using a standard calcium phosphate transfection technique *(12)*. Briefly, 1 μg of plasmid was mixed with 150 μL of 0.3*M* $CaCl_2$ and 2X HBS buffer and added to a single 6-well chamber. Six hours later, the medium was replenished. To assess the efficiency of recombination, a Cre-expressing adenovirus vector (AxCANCre, a gift from Dr. I. Saito) was applied to the culture thereafter at an MOI of 1 *(13)*. At various time-points, cells were dislodged, lysed, and β-galactosidase activity was measured by orthonitrophenyl-β-galactosidase assay (Invitrogen Corp., Carlsbad, CA) according to the manufacturer's instructions. Lysates were then subjected to Western analyses, either with anti-Rep (clone 303.9, Progen, Heidelberg, Germany) or anti-Cap (clone B1, Progen, Heidelberg, Germany), as reported previously *(4)*.

2.3. Development of Clones

Seven micrograms of each plasmid were used to transfect one 10-cm dish of 293 cells using a standard calcium-phosphate method at 70% of confluence. Forty-eight hours later, the cells were replated to several dishes and exposed to the selection medium containing both 800 μg/mL of G418 and 10 μg/mL of blasticidin S. The selection medium was replenished every 3 d. After 2 to 3 wk of selection, individual clones were recovered and amplified in 12-well plates in the presence of a half concentration of the selection medium of G418 and Blasticidin S. When a clone grew to semiconfluence in a 12-well plate, it was assumed to be established and was subjected to the analysis for packaging titer. The clones were numbered according to the order of establishment.

2.4. Titration of Vector Production

Established clones were further expanded, replated in new 12-well plates, then transfected with 0.5μg of the vector plasmid containing the *LacZ* gene cassette (driven by cytomegalovirus [CMV] promoter) flanked by two ITR sequences. Six hours after transfection, the medium was replenished, and Cre-expressing adenoviruses (AxCANCre) were added at an MOI of 1. Forty-eight hours later, cells were collected, subjected to three cycles of freeze–thawing, and treated with deoxyribonuclease I (Takara Bio, Inc., Ohtsu, Japan) for 30 min at 370°C as indicated by the manufacturer. The samples were quantified using dot-blot analysis. Known copy numbers of LacZ-expressing plasmid was used as controls.

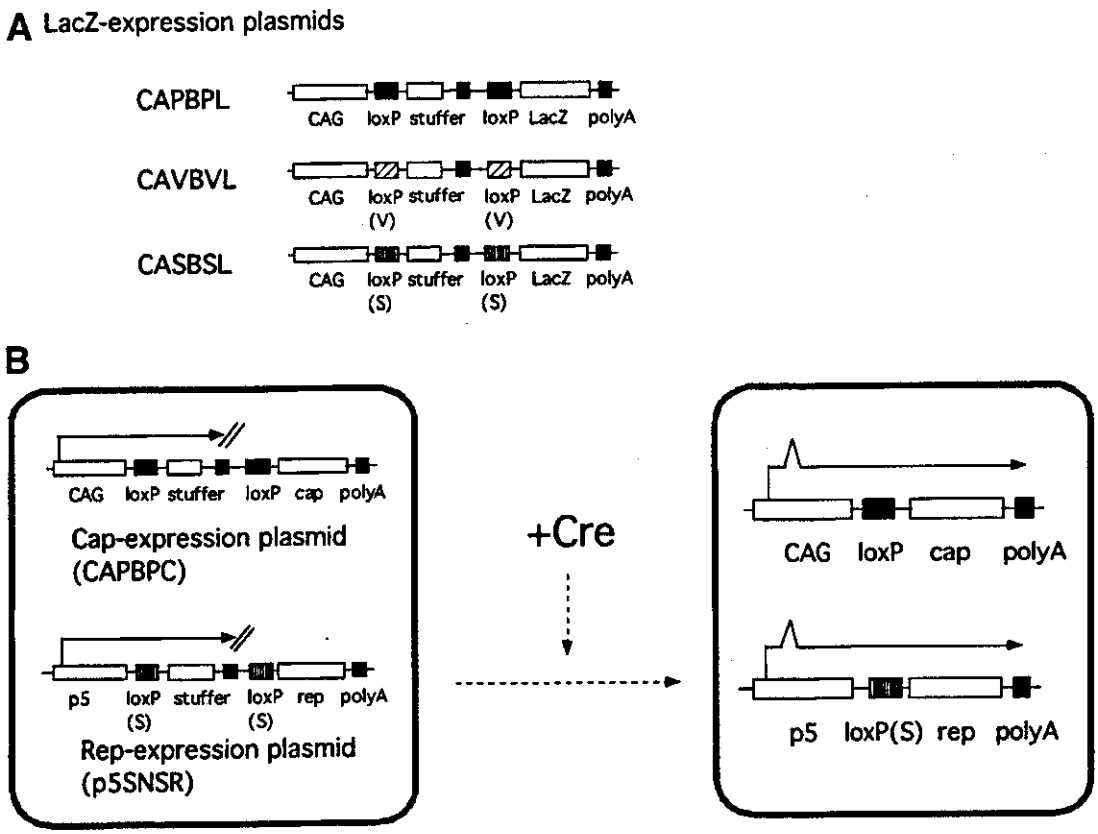

Fig. 1. Plasmid structure and the scheme of the cell line development. (**A**). To assess the recombination efficiency of the mutant loxP, three LacZ-expression plasmids are constructed. On infection with Ad-Cre, the stuffer sequences are removed with the efficiency depending on the wild-type or mutant loxP sequences, and the *LacZ* genes are driven by the CAG promoter. (**B**). The design of the cell line and the strategy for *rep* and *cap* expression are shown. To control *rep* and *cap* expression, a stuffer sequence is flanked by two loxP (wild-type or mutant) sequences. In the presence of Cre recombinase, the stuffer sequences are removed and the *cap* and *rep* genes are expressed.

2.5. Demonstration of Cre-Mediated Recombination by Polymerase Chain Reaction

Genomic deoxyribonucleic acid (DNA) was extracted from clone no. 3 by the standard techniques. Briefly, the recovered cells were treated with proteinase K, and total DNA was extracted with phenol chloroform. One microgram of total DNA was used as a template. A thermal cycler and the DNA polymerase ex-*Taq* (Takara Bio Inc., Ohtsu, Japan) were used for the PCR reaction according to the manufacturer's instructions. The forward primer sequences were 5'-TTC GGC TTC TGG CGT GTG AC-3' and 5'-TTG CGA CAT TTT GCG ACA CCA-3' for the *cap* and *rep* sequences, respectively. The reverse primer sequences were 5'-TCT GCG TAG TTG ATC GAA GCT-3' and 5'-GGG ACC TTA ATC ACA ATC TCG-3', respectively. The conditions for PCR were 940°C for 30 s, 560°C for 30 s, and 720°C for 1 min, and a total of 20 cycles of amplification were applied. The products were analyzed by agarose gel electrophoresis (0.8%) and visualized through ethidium bromide staining.

2.6. Statistical Analysis

The significance of the difference was estimated by Student's paired *t*-test.

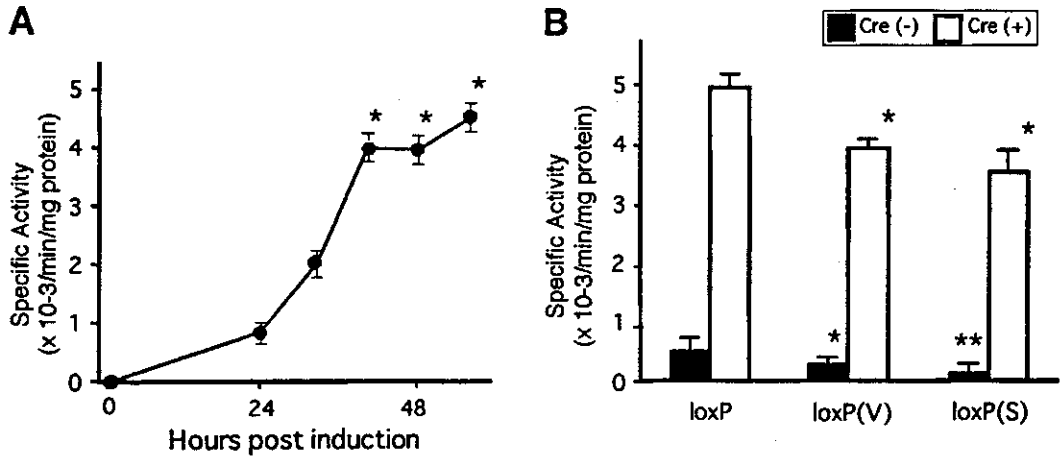

Fig. 2. Efficiency of recombination demonstrated in the wild-type and the mutant loxP. (A). Recombination activity of the wild-type loxP assessed at different time-points. The *asterisks* indicate the statistical significance ($p < 0.05$) of each data point against the nonindicated points. No significant differences were observed among the data points indicated by an asterisk. (B). Recombination efficiencies of wild-type and mutant loxP sequences. LacZ-expressing plasmids described in **Fig 1A** were used. Following transfection of the plasmids, 293 cells were infected by Ad-Cre at an MOI of 1. After 48 h, b-Gal activity was quantified. As for the baseline expression, values observed by loxP(V) were significantly lower than those with wild type as indicated by an *asterisk*. The baseline expression with loxP(S) was further significantly lower than that with loxP(V), as indicated by two *asterisks*. In terms of the expression levels following induction with Cre, values with both mutant loxPs showed significantly lower expression than those with wild type, as indicated by an *asterisk*. No differences were found in the values obtained by the mutant loxPs.

3. Results

3.1. Recombination Efficiency of Wild-Type and Mutant LoxP

To determine the optimal conditions for Cre–loxP-mediated induction of gene expression, we first examined the efficiency of recombination at various time-points. Recombination became significant at 40 h of induction by Ad-Cre and reached a plateau level thereafter (**Fig. 2A**). Therefore, we selected 48 h as a standard time-point for assessment of recombination. Then we compared the efficiency of recombination among the loxP sequences. The wild-type loxP showed the highest recombination efficiency, as assessed by LacZ expression (**Fig. 2B**). Therefore, we selected wild-type loxP for Cap expression plasmid. On the other hand, we selected the loxP (S) sequences for the Rep expression plasmids, as the basal level of expression was the lowest with this system.

3.2. Expression of Rep and Cap on Induction

Rep and Cap expression could be induced simultaneously by Cre recombinase (**Fig. 3**). Coexpression of the other protein inhibited the expression levels in both cases. The degree of Cap suppression was clearer than that of Rep suppression.

3.3. Development of Clones With Packaging Capacity

Following a period of 2–3 wk in selection medium containing both blasticidin S and G418, a total of 192 clones were chosen and amplified into 6-well culture plates. Of these, 22 clones reached semiconfluence in 10-cm dishes. These clones were further amplified, transfected with LacZ-expressing vector plasmids, and their ability to produce vector was determined. All of the 22 clones showed significant levels of vector production (**Table 1**). These LacZ-encoding vectors were capable of transducing 293 cells with similar effi-

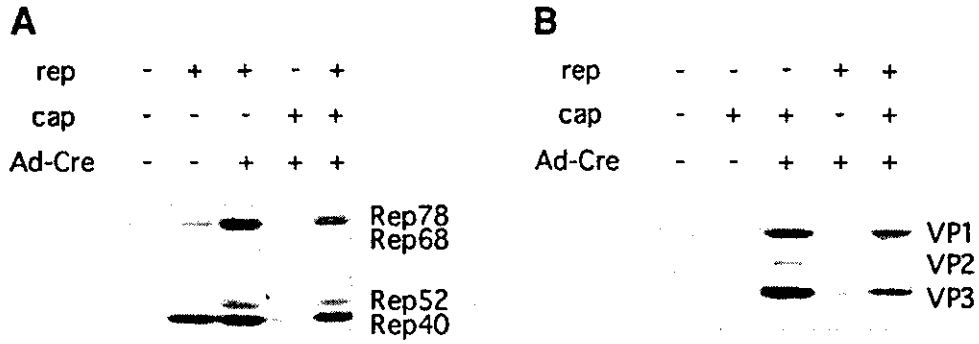

Fig. 3. *Rep* and *cap* expression profiles on treatment with Cre recombinase. One microgram of each plasmid was transfected into 293 cells in a 6-well plate. Following transfection, the cells received Ad-Cre and were lysed 48 h later. The cell lysates were analyzed by Western blotting using the monoclonal antibodies **(A)** 303.9 for *rep*, and **(B)** B1 for *cap*, respectively.

ciency to that made by the standard transfection method as assessed by conventional X-Gal staining (data not shown).

3.4. Stability of the Clones Developed

The established clones were further amplified and their stability was assessed at different time-points. As shown in **Table 1**, among the 22 clones developed, 6 continued to amplify for 2 wk. All of the expanded clones showed a significant packaging capacity. Of these, four clones tolerated additional expansion. These clones kept the growth speed of 293 cells, whereas the clones developed later (the higher numbered clones) tended to become slow growing. Of these, clone no. three maintained a significant packaging capacity throughout this period in terms of production of the AAV vector.

3.5. Detection of Cre-Mediated Recombination Events

Results of the analysis of clone no. 3 are shown in **Fig. 4**. PCR detection resulted in the amplification of the 1.1 and 1.2 kb for cap- and rep-expressing sequences within the untreated cells. Following Cre administration, shorter truncated sequences with 0.3 and 0.2 kb were amplified, suggesting simultaneous recombination events.

4. Discussion

In this study, we extended our previous findings *(4,5)* to regulate the expression of both *rep* and *cap* simultaneously, leading to development of a novel packaging cell line for the production of AAV vectors. Numerous attempts have been made to establish packaging cell lines, and sev-

Table 1
The Actual Titer of the Clones Obtained in This Study

Clone no.	0 Wk[a]	2 Wk	4 Wk
3	20.9[b]	11.6	15.0
8	15.3	6.7	1.3
10	11.3	4.4	0.4
11	0.7	—	—
12	31.5	2.4	2.8
15	2.5	—	—
17	5.2	—	—
22	2.9	—	—
25	3.4	—	—
27	7.5	—	—
28	15.0	12.5	—
31	1.6	—	—
33	6.7	—	—
34	5.5	—	—
35	7.7	—	—
36	2.6	—	—
38	10.6	—	—
40	2.9	—	—
41	5.8	—	—
44	10.9	11.1	—
57	4.4	—	—
60	1.8	—	—

[a]The time-point started when a clone grew to semiconfluence within a 10-cm dish. At that time, the clone was challenged for packaging titer. Clone no. 3 retained a significant packaging capacity throughout the study.
[b]Titers of AAV vector per 10-cm dish ($\times 10^9$)